Descriptions and Phylogenetic Relationships of the Guiana Shield Pencil Catfishes

by

Daniel R. Akin

A thesis submitted to the Graduate Faculty of
Auburn University
in partial fulfillment of the
requirements for the Degree of
Master of Science in Biology

Auburn, Alabama
August 6th, 2022

Trichomycterus, systematics, biogeography
South America, time-calibration

Copyright 2022 by Daniel Akin

Approved by

Dr. Jonathan Armbruster, Professor of Biology, Director of the Auburn University Museum of Natural History, and Curator of Fishes
Moisés Bernal, Assistant Professor of Biology
Dennis DeVries, Alumni Professor and Assistant Director for Research Programs

Abstract

The systematics of the catfish genus *Trichomycterus* Valenciennes 1832 are complicated and unresolved. This genus is paraphyletic, containing all members of the Trichomycterinae that cannot be adequately placed into an established genus due to the paucity of clearly defining characters that separated the lineages within this subfamily. The complete revision of *Trichomycterus* is a daunting task, and one that cannot be undertaken until most of the diversity within geographically relevant clades are described. This study describes six new species of *Trichomycterus* of the Pakaraima Mountains and nearby Kusad Mountain of the Guiana Shield region of South America. Additionally, I explore the phylogenetic relationships of these species and construct a time-calibrated phylogeny of the *Eremophilus* lineage within the Trichomycterinae. The results presented here suggest that there are two clades of *Trichomycterus* in the Guiana Shield, one species described in this study may constitute a species complex, that the diversification within the *Eremophilus* lineage occurred concurrently with the rise of the Andes Mountains, and that upper portion of the Ireng River may have flown north into the Grand Pakaraima River before being captured by the modern-day Rio Branco.

Acknowledgments

I'd like to acknowledge Aaron Geheber and Topher Hockaday, two colleagues and friends who provided a sounding board and without whom I may have never finished this thesis. Many museums and collectors deserve recognition, including Nathan Lujan, Erling Holm, and Marg Zur of the Royal Ontario Museum, David Werneke of the Auburn Museum of Natural History, Chris Taylor of the Illinois Natural History Survey, and all collectors of type material who are listed in the species accounts. I was not a part of the expeditions to collect this material, so I extend acknowledgments to all those involved, particularly Ovid Williams who has been instrumental in the cooperation between researchers and indigenous communities in Guyana as well as those indigenous communities who provided assistance to researchers. Additionally, I'd like to thank Malorie Hayes, Charles Stephan, Cori Black, Akila Abesinghe, Milton Tan, and Jamie Oaks for discussing ideas and methods presented in this thesis. I'd like to acknowledge Courtney Weyand and Matt Buehler, who were both kind enough to spend many hours priming me on molecular lab work and analyses. I'd like to thank my partner Taylor Papstein-Novak and my family Brad and Laura Akin, Tara Akin and Zach Torres, Ryan Akin and Sydney Shoemaker, whose continued love and support has guided me through the past few years. There are certainly people who I have accidentally omitted, and I wish to extend a blanket acknowledgement to all those who have helped me to accomplish this feat in some way or another.

Table of Contents

Abstract 2

Acknowledgments 3

List of Figures 5

List of Tables 6

List of Abbreviations 7

Phylogeny and Taxonomy of *Trichomycterus* 8

Introduction 8

Materials and Methods 15

Results 23

Taxonomic Accounts 24

Disussion 48

References 56

List of Figures

Figure 1 Linear Measurements Schematic 63

Figure 2 Vertebrae Counts 64

Figure 3 Osteological Characters 65

Figure 4 Gene Trees 66

Figure 5 Concatenated Tree 67

Figure 6 Time Calibrated Tree 68

Figure 7 Locality Map of Guiana Shield *Trichomycterus* 69

Figure 8 Hypothesized Paleo-Rivers of the Guiana Shield 70

Figure 9 Plate of Guiana Shield *Trichomycterus* 71

List of Tables

Table 1 Individuals used in phylogenetic analyses 72

Table 2 Primers used for PCR 77

Table 3 Lots used in morphological analyses 78

Table 4 Meristics of examined specimens 80

Table 5 Linear measurements of *Trichomycterus atoradorum* n. sp. 81

Table 6 Linear measurements of *Trichomycterus cooperwiti n*. sp. 82

Table 7 Linear measurements of *Trichomycterus gransabanensis* n. sp. 83

Table 8 Linear measurements of *Trichomycterus martincarteri* n. sp 84

Table 9 Linear measurements of *Trichomycterus ovidi* n. sp. 85

Table 10 Linear measurements of *Trichomycterus patamonorum* n. sp. 86

Supplementary Table 1 Comparison of *Trichomycterus guianensis* and *T. conradi* 87

List of Abbreviations

ROM	Royal Ontario Museum
AUMNH	Auburn Museum of Natural History
UCE	Ultra-Conserved Element
TSS	Traditional Sanger Sequencing
INHS	Illinois Natural History Survey
XML	Extensible Markup Language
NCBI	National Center for Biotechnology Information
MAFFT	Multiple Alignment using Fast Fourier Transform
DNA	Deoxyribonucleic Acid
PCR	Polymerase Chain Reaction
cs	Cleared and Stained Specimen
BI	Bayesian Inference
MCMC	Markov Chain Monte Carlo
ESS	Effective Sample Size
FBD	Fossilized Birth-Death Model

Introduction

The Trichomycteridae is a diverse family of Neotropical catfishes (Siluriformes) distinguishable from other catfishes chiefly by possession of opercular and interopercular odontodes and a pair of rictal barbels (see Baskin (1973), de Pinna (1989), or Fernández (2017) for a full diagnosis of the family). Trichomycteridae is distributed throughout most of South America and southern Central America (Fernández, 2017); some lineages are able to use their unique odontodes to aid in climbing waterfalls (Armbruster, 2011), allowing them to inhabit extreme reaches of headwaters as well as otherwise depauperate Andean mountain streams (Baskin, 1973). Most members of this family are general insectivores, but other members go to dietary extremes. Members of the subfamily Vandelliinae are sanguivorous parasites (Kelley & Atz, 1964; Machado & Sazima, 1983), feeding on blood from the gills of host fishes, while some members of the subfamily Stegophilinae feed on the mucus and scales of other fishes (Baskin *et al.*, 1980; Winemiller & Yan, 1989).

There are currently 374 valid species within Trichomycteridae, with the bulk of the species (273) belonging to the Trichomycterinae, 96 of which have been described only within the last ten years (Fricke *et al.*, 2022). Within this subfamily, there are currently nine recognized genera, *Bullockia* Arratia F. *et al.* 1978 (1 species), *Cambeva* Katz *et al.* 2018 (47 spp.), *Eremophilus* von Humboldt 1805 (1 sp.), *Hatcheria* Eigenmann 1909 (1 sp.), *Ituglanis* Costa & Bockmann 1993 (20 spp.), *Rhizosomichthys* Miles 1943 (1 sp.), *Scleronema* Eigenmann 1917 (10 spp.), *Silvinichthys* Arratia 1998 (7 spp.), and *Trichomycterus* Valenciennes 1832 (176 spp.), with the puzzling genus *Trichomycterus* being the focus of this thesis. *Trichomycterus* has been repeatedly shown to be paraphyletic (Ochoa *et al.*, 2017; Ochoa *et al.*, 2020; Fernández *et al.*, 2021). For the remainder of this thesis, I will refer to groupings within the Trichomycterinae as

the *Trichomycterus* Lineage and the *Eremophilus* Lineage (Ochoa *et al.*, 2020); both of these lineages contain members of the paraphyletic *Trichomycterus*. Our understanding of the taxonomy of Trichomycterinae is dubious at best, considering the large gaps in geographic sampling and short branches recovered in phylogenetic approaches. My goal is to establish a diagnosis for six new members of the *T. guianensis* clade of the *Eremophilus* lineage of the Trichomycterinae, including the first set of molecular loci for *Trichomycterus atoradorum* n. sp. Additionally, I explore the current limitations of time-calibrating phylogenies of the Trichomycteridae while providing a time-calibrated phylogeny for the *Eremophilus* lineage. My final goal is to combine the phylogenetic and morphological evidence with this time-calibration and the current understanding of South American geology to infer biogeographic relationships of Guiana Shield Rivers.

The colloquial name for many Trichomycterids in the is candiru, meaning pest (Baskin, 1973). It is likely, due to the parasitic nature of some trichomycterids, that many cultures had folk taxonomies and recognized members of the Trichomycteridae as a group. For the published record, however, Gill (1872) first recognized the Trichomycteridae as a family. The name Pygidiidae was also used early on, but a review by Tchernavin (1944) confirms that the proper family name is Trichomycteridae. The only species level revision of the family was completed by Eigenmann (1918). The seminal work of Baskin (1973) covers in-depth the history of the Trichomycteridae and *Trichomycterus* while providing one of the earliest attempts to bring phylogenetic hypotheses to Neotropical freshwater fishes, specifically members of the Trichomycteridae, but also providing phylogenetic hypotheses of relationships within Siluriformes, most of which have impressively stood the test of time and have been corroborated by advances in molecular phylogenetics (de Pinna, 2016).

Since Baskin's seminal work, de Pinna (1998) provided an update to the relationships within the Trichomycteridae, and concluded with a remark that the looming phylogenetic revision of *Trichomycterus* is "one of the most daunting challenges in the systematics of Neotropical siluriforms today" (p 300). This declaration is largely due to the genus *Trichomycterus* being a waste-basket genus, where members of the family lacking distinguishing characters are placed taxonomically until further review. This discouraging statement still rings true today; however, in the past five years, great strides have been taken in applying molecular phylogenetics to a large number of taxa within *Trichomycterus* (see Ochoa *et al.*, 2017; Katz *et al.*, 2018; Fernández *et al.*, 2021) although there is no clear revision of the genera of the Trichomycterinae.

Katz *et al.* (2018) erected the genus *Cambeva* based on the molecular data for only nine of 25 tentatively included members (now 47 members) and including osteological data of shared characteristics between *Cambeva* and its sister group, *Scleronema*, for 16 of 25 tentatively included members; however, Ochoa *et al.* (2020) reports the osteological characters used in this study to be incorrect, and doubles down on their previously stated notion that more sampling should be carried out before proposing changes to the genus-level classification (Ochoa *et al.*, 2017; Ochoa *et al.*, 2020). Additionally, Ochoa *et al.* (2020) called for clarification of the tricky history of the type species of *Trichomycterus*, *T. nigricans*. This has evidently been caried out in a historical review by Costa *et al.* (2019), providing evidence that the correct type locality of *T. nigricans* is not Santa Catarina state, Brazil, but actually the Rio Macacu basin, Rio de Janeiro state.

In addition to erecting *Cambeva*, Katz *et al.* (2018) proposed the separation of the Trichomycterinae into two clades – one clade comprised of the newly erected *Cambeva* sister to

Scleronema forming a group sister to *Trichomycterus sensu stricto* and another clade comprised of *Ituglanis,* other species of *Trichomycterus sensu lato*, *Bullockia* and *Eremophilus*. However, the separation of *Trichomycterus* here had no morphological basis. Ochoa *et al.* (2017; 2020) also recover similar clades, but do not recommend splitting *Trichomycterus* due to lack of morphological evidence and gaps in sampling. Costa (2021) provides comparative osteology for taxa within *Trichomycterus s.s.*, and even describes several subgenera, but does not provide character traits that separate this group from *Trichomycterus s.l.* This designation of *Trichomycterus s.s.* and *s.l.* is problematic as it leaves over twice as many species without a generic placement than would be done by creating a monophyletic *Trichomycterus s.s.* (Reis & De Pinna, 2022). Fernández *et al.* (2021) additionally proposed to synonymize the monotypic *Eremophilus* with *Trichomycterus*; however, this would result in even more confusion as *Eremophilus* (von Humboldt, 1805) would have priority over *Trichomycterus* (Valenciennes, 1832; Reis & De Pinna, 2022). Thus, the genus-level taxonomy of the Trichomycterinae is unsettled, in a state of flux, and there will likely either be multiple new genera described or synonymization of all taxa into one or a few genera, but such taxonomic decisions will need more work and are beyond the scope of this paper.

The current best understanding of deeper relationships within Trichomycteridae comes from a phylogenetic analysis of ultra-conserved elements (UCEs) amongst 139 taxa of Trichomycterids (Ochoa *et al.*, 2020). Traditional sanger sequencing (TSS) of multiple loci is a cheaper and simpler alternative to next generation sequencing, and, although it yields quantitatively less data, provides adequate data to demonstrate reciprocal monophyly of Trichomycterid species (e.g. Ochoa *et al.*, 2017; Katz *et al.*, 2018; Hayes *et al.*, 2020). Additionally, TSS is convenient for researchers adding new sequences to existing datasets using

previously implemented loci. Given the short branch lengths, wide geographic distribution, and general uncertainty surrounding the Trichomycterinae and *Trichomycterus*, both Ochoa (2020) and Fernandez et al. (2021) suggest that the current objective of researchers should be on phylogenetic studies of geographically distinct clades with thorough descriptions of species within these clades. Only after obtaining clear morphometric and molecular data for most of the representatives of each clade should a large effort of revision be made within the Trichomycterinae and *Trichomycterus* to alter the current classification and describe new genera.

The focus of this paper is on the *Trichomycterus guianensis* clade, sister to all clades excluding the *Eremophilus mutisii* clade within the *Eremophilus* lineage of trichomycterines (Ochoa *et al.*, 2020). The species within this clade inhabit the Guiana Shield region of South America. This area is of biogeographic interest for several reasons. It is hypothesized that river capture is a key contributor to the course of modern major rivers of South America, which is evident in the ongoing capture of the Orinoco headwaters by the Rio Negro via the Casiquiare Canal (Lundberg *et al.*, 1998; Winemiller *et al.*, 2008; Lujan & Armbruster, 2011). Additionally, a seasonal connection occurs between the Takutu and the Essequibo rivers over the Rupununi Wetlands in this region (Lujan & Armbruster, 2011; Souza *et al.*, 2012; de Souza *et al.*, 2020). Also, the hypothesized proto-Berbice river may have previously connected several rivers through this area, draining into the Atlantic by way of the modern Berbice, providing historical connections and recent isolations of freshwater fauna (Lujan & Armbruster, 2011). The highlands of the Guiana Shield also may have provided high-elevation refugia during historic marine incursions (Hubert & Renno, 2006). Finally, the Guiana Shield is incredibly old and mountainous in comparison to the young, lowland Amazon basin that neighbors it, and although much consideration has been given to the prehistorically recent Andean Orogeny for the

diversification of Neotropical freshwater fishes, the major lineages of freshwater fishes are much older than this event (Lundberg *et al.*, 1998). These factors create favorable conditions for a highly diverse fish fauna. Additionally, because this area is extremely difficult to reach and effectively sample, there are many species yet to be described (Lujan *et al.*, 2020).

Understanding the biogeography of the Guiana Shield is necessary to understand the ancient relationships among the major rivers of South America that are of ecological importance to thousands of species and of cultural and livelihood importance to many indigenous communities. These rivers are currently under threat from mining pollution by use of mercury for gold amalgamation as well as increased interest in the region's oil (Panelli, 2019; Montaña *et al.*, 2021). Understanding the history and future directions of these rivers may help guide difficult decisions that come with furthering development in these areas, such as decisions on irrigation, plumbing, hydroelectric, regulated fisheries, etc. (Winemiller *et al.*, 2016). The key to understanding the past of these rivers is implementing phylogenetic studies of small-bodied, positively rheophilic, headwater specialist species that have a wide geographic range (Lujan & Armbruster, 2011). The Trichomycteridae attests to each of these criteria (Fernández, 2017) and future studies of this group may very well provide answers to many paleogeographic puzzles concerning the rivers of South America. It should be made very clear that the first step towards realizing these goals is to achieve a fuller taxonomic coverage of the group in question, which is the goal of the present study.

The definition of a species has been subject to extensive discussion, debate, and review (see Mayden, 1997; Wheeler & Meier, 2000; de Queiroz, 2005; De Queiroz, 2007; Stankowski & Ravinet, 2021). For the remainder of this thesis, a species will be defined as satisfying at least two of the following criteria: 1. Genetic divergence 2. Morphological disparity 3. Distinct

geographic history. Oftentimes, data is missing for one of these criteria, therefore the combined approach implemented here allows for the application of at least two out of three of what I consider to be the most important variables for defining a freshwater fish species.

Hayes et al (2020) provided a phylogenetic analysis of several members of the *Trichomycterus guianensis* clade and concluded that there are two major clades within it. In addition to describing the taxa delimited in that study, I provide the first molecular data and description of a trichomycterid collected from a tributary to the Takutu River on Kusad Mountain in 2013. This study is the most extensive examination of Guiana Shield trichomycterids to date, combining molecular data with internal and external morphology of all *Trichomycterus* known from the Guiana Shield. There are limitations to this study, including lack of molecular data from *T. celsae*, *T. c.f. celsae*, *T. lewi*, and *T. gransabanensis* and lack of cleared and stained specimens (cs) of *T. celsae* and *T. c.f. celsae,* although there is one CT scan of the head of *T. c.f. celsae*, and a general lack of material for *T. celsae* (n = 1), *T. c.f. celsae* (n = 1), *T. guianensis* (n = 4, cs = 1), *T. gransabanensis* n. sp. (n = 3, cs = 1), and *T. lewi* (n = 0) all of which are rare in collections.

Materials and Methods

Molecular Data

Tissues of *Trichomycterus atoradorum* n. sp. were obtained from the Royal Ontario Museum (ROM) (see Table 1). I extracted whole genomic DNA using Qiagen DNeasy DNA Kit (QIAGEN Sciences Inc, Germantown, MD, USA). I amplified four genes, three of which (*16S, COI,* and *Cytb*) are mitochondrial and one of which (*rag2*) is nuclear. I selected these to maximize overlap between my samples and samples from previous works (Ochoa *et al.*, 2017; Hayes *et al.*, 2020) that would be included in downstream analyses. I amplified my target loci with polymerase chain reactions (PCR) using primer and protocols implemented by previous studies (see Table 2) (Ochoa *et al.*, 2017; Hayes *et al.*, 2020). The *16S* gene was amplified using the following primers and protocol: 16Sa-L and 16Sb-H (Palumbi & Baker, 1994); initial denaturation step of 180 s at 94 °C, then 30 cycles of denaturation (45 s at 95 °C), annealing (30 s at 54 °C) and extension (60 s at 68 °C), followed by a final extension of 60 s at 68 °C. The *COI* gene was amplified using the following primers and protocol: FishF1 and FishR1 (Ward *et al.*, 2005); initial denaturation step of 180 s at 94 °C, then 30 cycles of denaturation (45 s at 94 °C), annealing (30 s at 54 °C) and extension (60 s at 68 °C), followed by a final extension of 60 s at 68 °C. The *Cytb* gene was amplified using the following primers and protocol: CytbSiluF and CytbSiluR (Villa-Verde *et al.*, 2012); initial denaturation step of 180 s at 94 °C, then 30 cycles of denaturation (30 s at 94 °C), annealing (30 s at 52 °C) and extension (60 s at 72 °C), followed by a final extension of 300 s at 72 °C. The *rag2* gene was amplified using a two-step protocol. The first reaction was performed using the touchdown protocol described by Lovejoy & Collette (2001), with 164F and RAG2-R6 primers; initial denaturation step of 30 s at 95 °C, then 35 cycles of denaturation (30 s at 95 °C), annealing (60 s at 58, 56, 54, 52 °C) and extension (90 s at

72 °C), followed by a final extension of 300 s at 72 °C. The second PCR used 2 μL of template from the first run and the primers 176R and RAG2Ri (Oliveira *et al.*, 2011) in the following conditions: initial denaturation step of 30 s at 95 °C, then 35 cycles of denaturation (30 s at 95 °C), annealing (60 s at 58 and 60 °C) and extension (90 s at 72 °C), followed by a final extension of 72 °C for 300s. Primers used for PCR amplification were also used for DNA sequencing for all genes, with 176R and RAG2Ri being used for sequencing *rag2*. PCR products were visualized and size verified on a 0.8% agarose gel before samples were sent to GeneWiz (South Plainfield, NJ, USA) for purification, sample preparation and Sanger sequencing. Chromatographs from forward and reverse reads were imported into Geneious Prime v.11.0.14 (Kearse *et al.*, 2012) for assembly.

I downloaded additional sequence data from previous studies for members of the *Trichomycterus guianensis* clade from the NCBI Genbank (see Table 1) (e.g. Ochoa *et al.*, 2017; Hayes *et al.*, 2020). Lastly, alignments for a concatenated dataset including taxa from the *Eremophilus* lineage, as well as representative members of clades within the *Trichomycterus* lineage, and members of the Stegophilinae and Vandellinae as an outgroup were imported if three of four loci for that individual could be accessed from GenBank, with the exception of two individuals of *T. conradi* (AUFT10213 and AUFT10294; *16S* and *Cytb* only), which is a focal taxon of this study.

Phylogenetic Analysis

Assembled consensus sequences were aligned using the MAFFT algorithm (Katoh *et al.*, 2002), and visually assessed within Geneious Prime. Alignments were trimmed to the following lengths for consistency with previously published sequences (Ochoa *et al.*, 2017; Hayes *et al.*, 2020): *16S*, 466 bp; *COI*, 521 bp; *Cytb*, 858 bp; and *rag2*, 885 bp. Individual gene trees of the *T.*

guianensis clade were analyzed with *Scleronema minutum* as an outgroup to assess whether individual genes can be used for barcoding (e.g. Reis & De Pinna, 2022) and to inform biogeographical discussion of topologies estimated with different rates of diversification. The concatenated dataset (2730 bp) was analyzed with all taxa fitting the prior criteria (n = 123).

I estimated gene trees using a Bayesian Inference (BI) approach in the program MrBayes v3.2.6 via the CIPRES web portal (Huelsenbeck & Ronquist, 2005; Miller & Pfeiffer, 2010). Protein coding genes were partitioned by codon position and substitution models were simultaneously estimated using the lset function (Huelsenbeck & Ronquist, 2005). The concatenated analysis was similarly partitioned by both gene and codon position. For all gene tree analyses, I used a Markov Chain Monte Carlo (MCMC) to sample the posterior for $2*10^7$ generations. To ensure the chains converged and to reduce auto-correlation among samples, I performed two independent runs with four chains (three heated, one cold). I sampled tree topologies from the posterior every 1000 generations. For the concatenated tree analysis, I used a MCMC to sample the posterior for $1.5*10^7$ generations. I performed two independent runs with four chains and sampled tree topologies from the posterior every 1000 generations. The posterior and trees were summarized in MrBayes v3.2.6 using the default 25% burn-in. To ensure that each of the MCMC runs had sufficient mixed for all estimated parameters, I used the program Tracer v1.7 to visualize posterior sampling and calculate estimated sample sizes for each parameter. Parameters with ESS > 200 were considered to have converged (Rambaut *et al.*, 2018). The parameters and trees were summed in MrBayes v3.2.6 using the default 25% burn-in. The resulting 50% majority consensus rule phylogeny is reported and support is reported in posterior probabilities. Values greater than or equal to 95 are considered strong support, values from 75 to 95 are considered weak support, and any value less than 75 is not supported.

Time-Calibration

Taxa included in the time-calibrated phylogeny were all sequences of the *Eremophilus* Lineage that met the criteria for the above concatenated analysis. Any taxa that were not a part of the *Trichomycterus guianensis* clade, but had multiple nearly identical alignments were trimmed to have only one representative, prioritizing alignments that contained all four loci. I included the only fossil that has been confirmed as a member of the Trichomycteridae as a primary calibration (Bogan & Agnolin, 2009), and although it cannot be accurately diagnosed using morphology to a generic level, I make an assumption that it belongs to the *Eremophilus* lineage (most likely the *T. areolatus* clade) based on biogeographic hypotheses described by Bogan & Agnolin (2009). This fossil was discovered in the Monte Hermosa formation, which is aged 4.5–5.3 Ma (Tomassini *et al.*, 2013). I estimated the time-calibrated phylogeny under a Fossilized Birth Death (FBD) model in BEAST v2.6 (Stadler, 2009; Bouckaert *et al.*, 2014; Heath *et al.*, 2014; Barido-Sottani *et al.*, 2018). The FBD model approach is optimal for the *Eremophilus* lineage because it allows for a primary calibration and fossils do not need to be assigned to a specific node, rather the fossil can be treated as a tip in in the entire tree or constrained to an *a priori* clade within the data and integrates the fossil occurrence times into the tree prior (Heath *et al.*, 2014). I used the program BEAUTi to assign model parameters and generate the XML input file for BEAST (Bouckaert *et al.*, 2014). I partitioned my data by gene and protein coding genes were partitioned by codon according to the following scheme: (1,2) + 3. To treat my fossil as a tip, I toggled the tip dates parameter and assigned the fossil taxon as a tip dated 5.2 Ma. Substitution rates for codon positions and 16S were estimated simultaneously using the program BmodelTest (Bouckaert & Drummond, 2017). I used an uncorrelated lognormal relaxed molecular-clock with default values. I set the following parameters required to estimate divergence times under the

FBD model. To create a proper prior distribution for the clock prior, we set the ucldMean to an exponential prior density with a mean of ten. The parameters for the tree prior are diversification rate, turnover, sampling proportion, and rho (the proportion of sampled extant species). I used a normal prior restricted on the interval [0.01, 0.19] for diversification rate based on the estimated diversification rate of Neotropical Otophysan fishes from (Miller & Román-Palacios, 2021; Miller & Román-Palacios, n.d.). I used an uninformative prior (i.e. uniform [0, 1]) for turnover as it is difficult to calculate and related to derivations of the other parameters (Barido-Sottani *et al.*, 2018). I used an exponential prior with a mean of 0.2 on the interval [0, 1] for sampling proportion (i.e. the likelihood of sampling a fossil of an extant taxa within the *Eremophilus* lineage is probably low when considering only one fossil has been recovered for what is over 120 presently described extant species). Finally, for rho I used a beta prior (alpha = 10, beta = 20, [0.01,0.99]) based on the assumption that roughly 33% ([17.9%, 47.9%; 95%CI]) of all extant species (including those undescribed) within the *Eremophilus* lineage are included in this tree. Additionally, I constrained the monophyly of all *Eremophilus* lineage members excluding the *E. mutisii* clade, making that clade the outgroup for this analysis. The complete XML file can be found in the supplementary materials. Two independent (MCMC) chains were run for $5*10^7$ generations. I sampled parameters and trees every 2500 generations. I checked sufficient mixing of parameters (ESS>200) for both independent runs as well as the combined run using Tracer v1.7 (Rambaut *et al.*, 2018). I combined trees from both runs using LogCombiner v1.10.4 with a 10% burn-in resampled at an interval of 5000 (Suchard *et al.*, 2018). Because the fossil was only used to inform the FBD model and could attach to any lineage, I then pruned it off using the FullToExtantTreeConverter plug-in in BEAUTi (Bouckaert *et al.*, 2014; Barido-Sottani *et al.*, 2018). I input combined trees into TreeAnnotater v1.10.4 to obtain the maximum credibility tree

and posterior probabilities (Suchard *et al.*, 2018). I then visualized the tree with a geological timescale in R (R Core Team, 2022) using the *strap* package (Bell & Lloyd, 2015). Support for relationships is assessed with posterior probabilities. Values greater than or equal to 95 are considered strong support, values from 75 to 95 are considered weak support, and any value less than 75 is not supported.

Morphological Data

All type material and comparative material was obtained from ROM, the Illinois Natural History Survey (INHS) and the Auburn Museum of Natural History (AUMNH). Measurements and meristics compared to original descriptions of *T. lewi* and *T. celsae* when necessary (Lasso & Provenzano, 2002). Material examined is as follows: *Trichomycterus guianensis* (Eigenmann, 1909): AUM 62932, 1, 109.3 mm SL; AUM 62938, 1, 35.9 mm SL; AUM 63677, 3 (1 cs), 43.1-75.8 mm SL; ROM 78137, 1, 20.2 mm SL. *Trichomycterus conradi* (Eigenmann, 1912): AUM 67194, 1, 44.9 mm SL; ROM 91436, 9 (1 cs), 23-41.7 mm SL. *Trichomycterus celsae* (Lasso & Provenzano, 2002): AUM 63676, 1, 49.4 mm SL. *Trichomycterus atoradorum* n. sp.: ROM 95880, 7 (1 cs), 51.1-82.1 mm SL. *Trichomycterus patamonorum* n. sp.: AUM 28148, 4, 60.8-97.9 mm SL; AUM 35585, 5, 30–53.7 mm SL; AUM 35590, 5, 29.8-51.7 mm SL; AUM 45167, 1, 83.4 mm SL; AUM 45399, 9, 37.3-101.9 mm SL; AUM 62733, 13 (2 cs), 74.6-100.3 mm SL; AUM 62742, 1, 63.6 mm SL; AUM 62748, 10, 58.3-72.8 mm SL; AUM 62754, 7, 54.4-94.2 mm SL; AUM 62802, 10, 73.9-85.3 mm SL; AUM 62812, 3, 38-47.1 mm SL; AUM 62902, 14 (2 cs), 51.5-62.7 mm SL; AUM 62910, 9 (2 cs), 35.3-100.5 mm SL; AUM 62935, 1, 34.1 mm SL; INHS 49567, 3, 68.1-101.7 mm SL; ROM 83790, 6, 39.8-74.3 mm SL; ROM 83804, 2, 51.6-79.3 mm SL; ROM 89590, 1, 54.4 mm SL; ROM 89618, 1, 62.6 mm SL; ROM 89696, 1, 50.7 mm SL; ROM 89716, 1, 56.1 mm SL; ROM 89932, 6, 64.3-93.5 mm SL; ROM 89940, 2, 30.5-

50.5 mm SL; ROM 91352, 18, 55.7-88 mm SL; ROM 91493, 1, 74 mm SL; ROM 93441, 6, 44-59 mm SL; ROM 93451, 3, 40–50.7 mm SL; ROM 93459, 1, 44.7 mm SL; ROM 93482, 1, 50.4 mm SL; ROM 93511, 1, 72.9 mm SL; ROM 93526, 1, 38 mm SL; ROM 93539, 4, 50.4-67.5 mm SL; ROM 94991, 2, 44.8-59.6 mm SL; ROM 95000, 2, 36.8-38.5 mm SL; ROM 95076, 1, 31.6 mm SL; AUM 36615, 6, 34.9-79 mm SL; AUM 36653, 1, 36.5 mm SL; AUM 36680, 5, 26.4-32.8 mm SL; AUM 36681, 12 (2 cs), 22.2-54.1 mm SL. *Trichomycterus gransabanensis* n. sp.: AUM 36634, 4 (1 cs), 25.6-66.5 mm SL. *Trichomycterus martincarteri* n. sp.: ROM 83791, 6 (1 cs), 23.6-70.8 mm SL; ROM 83818, 1, 70.7 mm SL; ROM 83833, 3, 40.2-68.9 mm SL; ROM 83834, 2, 57.6-59.7 mm SL; ROM 83842, 2, 65-75.6 mm SL; ROM 89625, 1, 54.5 mm SL; ROM 89627, 1, 40.4 mm SL; ROM 89685, 1, 36.4 mm SL; ROM 89717, 2, 39.9-54.1 mm SL; ROM 89725, 1, 46.7 mm SL; ROM 93437, 2, 43.4-63.3 mm SL; ROM 93441, 2 (1 cs), 55.2-61 mm SL; ROM 93457, 1, 61.8 mm SL; ROM 93469, 1, 42.9 mm SL; ROM 93512, 1, 70.5 mm SL; ROM 93515, 4, 57.4-68.1 mm SL; ROM 93539, 1, 60.4 mm SL; ROM 93542, 1, 72.2 mm SL. *Trichomycterus ovidi* n. sp.: AUM 62949, 13 (2 cs), 37.3-134.7 mm SL. *Trichomycterus cooperwiti* n. sp.: AUM 67072, 1, 24.5 mm SL; AUM 67098, 1, 28.9 mm SL; AUM 67129, 17 (1 cs), 25.1-53.9 mm SL; AUM 67138, 3, 25.7-28.1 mm SL; AUM 67154, 1, 43.9 mm SL; AUM 67172, 4, 33-77 mm SL; AUM 67179, 2, 35.2-62.1 mm SL; AUM 67200, 1, 31 mm SL. *Trichomycterus c.f. celsae*: AUM 36672, 1, 36.4 mm SL.

Morphometric data were recorded following de Pinna (1992) using digital calipers (0.01 mm) (Figure 1). Uppercase roman numerals refer to unbranched rays, and lowercase roman numerals refer to unbranched, unsegmented rays that can only be counted in cleared and stained specimens. Caudal-fin ray counts are reported as upper lobe + lower lobe. Vertebrae numbers did not include those involved in the Weberian complex, and the compound caudal centrum was

counted as one element. Additionally, I report the number of vertebrae with neural/hemal spines adjacent with and posterior to the anterior-most dorsal and anal pterygiophores (including the vertebrae with a neural/hemal spine directly anterior to the anterior-most pterygiophore). Finally, I also report the number of vertebrae with neural/hemal spines adjacent with and posterior to the anterior most procurrent ray (Figure 2). Vertebrae counts and osteological data were obtained from cleared and stained specimens (Taylor & Van Dyke, 1985) following nomenclature from de Pinna (1989) as well as CT scans available from MorphoSource (Figure 3). Meristic and morphometric data were recorded on the left side of specimens whenever possible.

Results

Phylogeny and Time-Calibration

The gene trees consistently recovered the reciprocal monophyly of all species except for *T. conradi*, albeit with topological discordance at the deep nodes among the trees (Figure 4). For *T. conradi*, one individual from the Potaro drainage had an unresolved relationship with the individuals from the Ireng in both the *16S* analysis and the *rag2* analysis, but reciprocal monophyly was recovered in the *COI* analysis. For the *16S* analysis, strong support was recovered for a clade containing *T. martincarteri* n. sp., *T. atoradorum* n. sp., and *T. patamonorum* n. sp. (pp = 95%), but the relationship between *T. atoradorum* n. sp. and *T. patamonorum* n. sp. is not well supported. The *COI* analysis recovers *T. atoradorum* n. sp. in a polytomy with with *T. conradi* and an unresolved grouping of *T. guianensis* and *T. cooperwiti* n. sp. For the *Cytb* analysis, *T. atoradorum* n. sp. is recovered as sister to all other clade-members (pp = 100%). The only nuclear gene tree, based on *rag2*, recovers *T. atoradorum* n. sp. in a polytomy with *T. conradi* (Ireng) and a well-supported (pp = 100%) clade of *T. ovidi* n. sp. sister to a well-supported (pp = 100%) sister group of *T. guianensis* and *T. cooperwiti* n. sp.

The concatenated analysis recovered two subclades within the *T. guianensis* clade (pp = 99%) (Figure 5). One subclade consists of *T. patamonorum* n. sp. sister to *T. martincarteri* n. sp. (pp = 100%), with an unresolved relationship to *T. conradi* (pp = 66%), with *T. atoradorum* n. sp. sister to all members of the subclade (pp = 95%). The other subclade strongly supports a sister relationship of *T. guianensis* and *T. cooperwiti* n. sp. (pp = 100%) with *T. ovidi* n. sp. sister to that grouping (pp = 100%). For the deeper relationships in the *Eremophilus* lineage, the *T. chapmani* clade is recovered sister to all remaining Trichomycterines, which are in a polytomy of the *T. banneaui* clade + *T. areolatus* clade + *T. sp. JM* + *Trichomycterus* sp. 2, and the genus

Ituglanis, and the *T. guianensis* clade + *E. mutisii* clade + *T. punctulatus* clade + the *Trichomycterus* lineage. Backbone support values are not resolved with this dataset.

The time-calibration recovered a different topology within the *Trichomycterus guianensis* clade. In this analysis, *T. conradi* is firmly placed within the subclade consisting of *T. patamonorum* n. sp., *T. martincarteri* n. sp., and *T. atoradorum* n. sp. (pp = 99%) as sister to all remaining members of the subclade (pp = 97%) The estimates of the time-calibration place the oldest divergence within the *Eremophilus* lineage at 18.48 Ma ([5.52, 37.57] 95% HPD). The focal group of this study, the *T. guianensis* clade, is estimated to have diverged at 17.37 Ma ([5.02,35.04] 95% HPD), with the two subclades diverging at 14.69 Ma ([3.93, 30.2] 95% HPD). *Trichomycterus atoradorum* n. sp. is estimated to have diverged 9.4 Ma ([2.14, 20.25] 95% HPD).

Taxonomic Accounts

***Trichomycterus atoradorum*, new species**

Holotype: Ex ROM 95880, 57.9 mm SL, Guyana; Upper Takutu-Upper Essequibo (Region 9), Unnamed Tributary of Dabarwau Creek, Takutu River drainage, Amazon River basin, 2.811967, -59.86667; D.C. Taphorn, M. Kolmann, M. Ignace, L. Kalicharan, 23 October 2013.

Paratypes: ROM 95880, 6 (1 cs) 51.1–82.1 mm SL, same information as holotype.

Diagnosis: *Trichomycterus atoradorum* is distinguishable from all other Guiana Shield *Trichomycterus* by unique pattern, with mostly solid horizontal stripe originating from opercular odontodes and following lateral line through medial caudal fin rays, bordered dorsally by one or two horizontal rows of stippling, which is bordered dorsally by another solid horizontal stripe that terminates into horizontal line of spots when approaching area of dorsal-fin base, which is bordered dorsally again by a horizontal row of stippling (vs. no stripes and body coloration either entirely plain or with small or large spots or blotches). It is also distinguishable from *T. guianensis*, *T. gransabanensis*, *T. cooperwiti*, and *T. martincarteri* by having I8–9 pectoral fin rays (vs. I6–7). *Trichomycterus atoroadorum* is also distinguishable from *T. lewi* by having 36 vertebrae (vs. 33), and 14 and 15 ventral and dorsal procurrent rays respectively (vs. 10–11 and 12–13). *Trichomycterus atoroadorum* n. sp. is also distinguishable from *T. patamonorum* n. sp. by having 36 vertebrae (vs. 33–34), and 14 ventral procurrent rays (vs. 10–11).

Description: Measurements and external meristics based on six specimens, internal meristics based on one cleared and stained specimen (see Tables 4 and 5). Species apparently small, largest specimen 82 mm SL. Predorsal profile of body convex dorsally and mostly flat ventrally, with dorsal portion flattening out in postdorsal region. Caudal peduncle tapers slightly posteriorly, creating uppercase *U*, but procurrent caudal-fin rays remain flat with posterior

profile of body, giving entire caudal region rectangular appearance. Corners of caudal fin only slightly rounded, flat on posterior edge, contributing to rectangular shape of caudal region. Head trapezoidal from dorsal view and triangular from lateral view, compressing anteriorly in both views. Eyes dorsal, equidistant from nape and anterior edge of premaxilla, small and round. Subterminal mouth, nearly as wide as extent of anterior edge of head. Bottom lip fleshy. Upper and lower lip joined by fleshy corner. Upper lip with minute papillae and extending into maxillary and rictal barbels just anterior to connection with bottom lip. Barbels all wider at base and narrowing distally. Maxillary barbel slightly longer than nasal barbel, both much longer than rictal barbel. All barbels much longer than snout length.

Pectoral fins with flat posterior edge and slightly rounded on leading edge, almost triangular in shape, with long filamentous extension of spine almost doubling length of fin. Pectoral-fin rays usually I,8 (4) or I,9 (3). Pelvic fins longer than wide, leading edge curved, posterior edge also curved, originating well anterior to dorsal fin insertion, almost at middle of standard length (mean = 56.9%). Pelvic-fin rays I,4 (7). Dorsal fin originating near posterior third of standard length (mean = 65.3%). Dorsal fin with three unbranched unsegmented rays in cleared and stained specimens (iii, not visible in whole specimens): remaining dorsal-fin rays II,7 (6) or I,7 (1). Anal fin originating posterior to dorsal fin. Anal fin with three unbranched unsegmented rays in cleared and stained specimens (iii, not visible in whole specimens): remaining anal-fin rays II,5 (7). Caudal fin rays I,5 + 6,I. Anus approximately equidistant to origin of pelvic fins and origin of anal fin.

Interopercular odontode patch with 40–49 odontodes; opercular odontode patch with 18–24 odontodes. Thirty-six vertebrae, with 20 posterior to dorsal fin, 16 posterior to anal fin, and 7 posterior to anterior-most procurrent ray (1 cs). Dorsal procurrent rays 14; ventral procurrent

rays 15 (1 cs). Parurohyal robust, metapterygoid rhomboidal, coming to posterodorsal point and dorsomedial point. Supraoccipital foramen long and disconnected from very small anterior foramen. Sphenotic process directed anterolaterally. Pelvic girdle slender. Posteroventral edge of opercle nearly straight. Posttemporo-supracleithrum with long thin anterodorsal process. Dorsal ural process short and thick with anterior notch near base.

Coloration: Cream-colored ventrally gradually becoming light brown dorsally with dark brown patterning. Pattern is mostly solid horizontal stripe with soft edges originating from opercular odontodes and following lateral line through medial caudal-fin rays interrupted by brief break in coloration at peduncle, bordered dorsally by one or two horizontal rows of stippling, stippling bordered dorsally by solid horizontal stripe that terminates into horizontal line of spots when approaching area of dorsal-fin base, dorsal stripe bordered dorsally by horizontal row of stippling. Additional randomized stippling on lateral surface of body and caudal fin. Dark brown macula on opercular odontode patch larger than patch, and dark brown macula anterior to interopercular odontode patch. Neurocranial region of head darker than rest of head with unorganized stippling distally reaching maculae of odontode patches.

Remarks: *Trichomycterus atoradorum* is has only been found on Kusad Mountain which is a high area surrounded by savanna, far isolated from the Pakaraima Mountains where all other Guiana Shield *Trichomycterus* are known. This allows for more straightforward biogeographical interpretations given the simplicity of the locality, as any synapomorphies seen in related Pakaraima *Trichomycterus* would provide support for a common ancestor in the proto-Berbice paleo-drainage. This species is most similar in form to *T. patamonorum*, which is wide ranging and phylogenetically closely related to *T. atoradorum*. These two (along with the one known

representative of *T. c.f. celsae*) are the only known Guiana Shield *Trichomycterus* to occasionally have I,9 pectoral-fin rays.

Distribution: *Trichomycterus atoradorum* is known from only one locality on Kusad Mountain, south of the village Shulinab, which flows into the Takutu River on the Guyana/Brazil border.

Etymology: *Atoradorum* is the Latin plural neuter genitive of Atorad. It is named for the Atorad indigenous people that once inhabited the region and have since been assimilated into the Wapichan Nation.

***Trichomycterus cooperwiti*, new species**

Holotype: To be designated.

Paratypes: All collections Guyana, Potaro-Siparuni Region 8, tributary to Branco River, Negro River drainage, Amazon River basin: AUM 67072, 1, 24.5 mm SL, Branana Rapids downstream of Orinduk Falls, Ireng River, 4.67585, -60.06046, D.C. Werneke, J.W. Armbruster, D.I. Brooks, M. Ram, 4 January 2016; AUM 67098, 1, 28.9 mm SL, Guyana, Potaro-Siparuni Region 8, Tumong Creek left-hand tributary of Ireng River, Ireng River, tributary to Branco River, Negro River drainage, Amazon River basin-Tumong Creek left-hand tributary of Ireng River, 4.71971, -60.01311, D.C. Werneke, J.W. Armbruster, D.I. Brooks, M. Ram, 6 January 2016; AUM 67129, 17, 25.1–53.9 mm SL, Guyana, Potaro-Siparuni Region 8, Sukwabi Creek at the top of Andu Falls, Ireng River, 5.08955, -59.97514, N.K. Lujan, J.W. Armbruster, D.C. Werneke, M. Ram, D.I. Brooks, 9 January 2016; AUM 67138, 3, 25.7–28.1 mm SL, Guyana, Potaro-Siparuni Region 8, shoals at the mouth of Monkey Creek, Ireng River, 5.04398, -59.97717, N.K. Lujan, J.W. Armbruster, D.C. Werneke, 9 January 2016; AUM 67154, 1, 43.9 mm SL, Guyana, Potaro-Siparuni Region 8, Ireng River above Uluk Tuwuk Falls, 5.08388, -59.98762, D.C. Werneke,

N.K. Lujan, J.W. Armbruster, D.I. Brooks, M. Ram, 11 January 2016; AUM 67172, 4, 33–77 mm SL, Guyana, Potaro-Siparuni Region 8, Sukwabi Creek at the top of Andu Falls, Ireng River, 5.08955, -59.97514, J.W. Armbruster, N.K. Lujan, D.I. Brooks, M. Ram, 12 January 2016; AUM 67179, 2, 35.2–62.1 mm SL, Guyana, Potaro-Siparuni Region 8, Shoals at the mouth of Monkey Creek, Ireng River, 5.04398, -59.97717, J.W. Armbruster, N.K. Lujan, D.I. Brooks, 12 January 2016; AUM 67200, 1, 31 mm SL, Guyana, Potaro-Siparuni Region 8, Ireng River at Sand Hill shoals, 4.96554, -59.99411, D.C. Werneke, J.W. Armbruster, N.K. Lujan, M. Ram, D.I. Brooks, 14 January 2016.

Diagnosis: Distinguished from *T. conradi*, *T. celsae*, and *T. ovidi* by spots present (vs. absent). Distinguished from *T. atoradorum* and *T. patamonorum* by pectoral-fin ray count I,6–7 (vs. I,8–10). Distinguished from *T. patamonorum* by caudal fin shape truncate (vs. emarginate). Distinguished from *T. lewi* by having 37 vertebrae (vs. 35). Distinguished from *T. guianensis* and *T. gransabanensis* by having 37 vertebrae (vs. 39 and 38 respectively), 15 ventral procurrent rays (vs. 25 and 21 respectively), and 26 dorsal procurrent rays (vs. 39 and 30 respectively). Distinguished from *T. martincarteri* by having 18 vertebrae posterior to the anal fin (vs. 17), by having 12 vertebrae posterior to the anterior-most procurrent ray (vs. 9–10), and by having 26 dorsal procurrent rays (vs. 21–22).

Description: Measurements and external meristics based on 29 specimens, internal meristics based on one cleared and stained specimen (see Tables 4 and 6). Species small, largest specimen 77 mm SL. Predorsal profile of body convex dorsally and mostly flat ventrally, with dorsal portion flattening out in postdorsal region. Caudal peduncle tapers slightly posteriorly, creating uppercase *U*, but procurrent caudal-fin rays remain flat with posterior profile of body, caudal-fin rays extend dorsoventrally deeper than procurrent rays giving entire post-dorsal region

rectangular appearance with flared base at caudal fin. Edges of caudal fin only round slightly before coming to corner, posterior edge convex, caudal fin rounded to truncate. Head trapezoidal from dorsal view and triangular from lateral view, compressing anteriorly in both views. Eyes dorsal, nearer to anterior edge of premaxilla than nape, small and round. Subterminal mouth, nearly as wide as extent of anterior edge of head. Upper and lower lip joined by fleshy corner. Upper and lower lip with minute papillae. Upper lip extending into maxillary and rictal barbels just anterior to connection with bottom lip. Barbels all slightly wider at base and narrow only slightly distally. Maxillary barbel equal to or slightly longer than nasal barbel, both much longer than rictal barbel. All barbels longer than snout length.

Pectoral fins with flat posterior edge and rounded on leading edge, with long filamentous extension of spine roughly half as long as spine length. Pectoral-fin rays usually I,7 (17), I,6,I (9), or I,6 (4). Pelvic fins longer than wide, leading edge curved, posterior edge also curved, originating anterior to dorsal fin insertion, almost at middle of standard length (mean = 53.1%). Pelvic-fin rays I,4 (26), I,3,I (3), or II,2,I (1). Dorsal fin originating before posterior third of standard length (mean = 62.7%). Dorsal fin with three unbranched unsegmented rays in cleared and stained specimens (iii, not visible in whole specimens): remaining dorsal-fin rays II,7 (25), II,6,I (2), II,6 (1), II,8 (1), or I,8 (1). Anal fin originating posterior to dorsal fin. Anal fin with three unbranched unsegmented rays in cleared and stained specimens (iii, not visible in whole specimens): remaining anal-fin rays II,5 (16), I,6 (9), II,6 (4), or II,4 (1). Caudal fin rays I,5 + 6,I. Anus roughly equidistant from origin of anal fin to origin of pelvic fins.

Interopercular odontode patch with 17–30 odontodes; opercular odontode patch with 10–15 odontodes. Vertebrae count 37, with 21 posterior to dorsal fin, 18 posterior to anal fin, and 12 posterior to anterior-most procurrent ray (1 cs). Dorsal procurrent rays 26; ventral procurrent

rays 15 (1 cs). Parurohyal short, metapterygoid large and irregular, with deep posterior notch. Supraoccipital foramen long, thicker anteriorly, and disconnected from rounded anterior foramen. Sphenotic process directed anterolaterally. Pelvic girdle with one sharp anteromedial processes and lateral notch. Posteroventral edge of opercle slightly concave. Posttemporo-supracleithrum with long thin anterodorsal process. Dorsal ural process short and thick.

Coloration: Cream colored ventrally gradually becoming dark brown dorsally with darker brown patterning. Spots mostly circular, but some slightly blotchy. One horizontal row of spots following the lateral line, often forming dashes comprised of overlapping spots, appearing as a mostly solid line in the smallest individuals. Smaller stippling alongside larger spots near the head. Head dark, darkest in the neurocranial region. Upper and bottom lips pigmented.

Distribution: Restricted to the upper Ireng River of the Branco River drainage. Known from the Ireng, Sukwabi, and Monkey rivers, and Tumong Creek.

Etymology: Named for the grandson of Dr. Lawrence Wit in honor of Dr. Wit's generous support of the Auburn University Museum of Natural History and Cooper's great interest in the museum and biology.

***Trichomycterus gransabanensis*, new species**

Holotype: Ex AUM 36634, 66.5 mm SL, Venezuela, Bolivar State; Unnamed Tributary to Yuruani River, tributary to Kukunan River, Caroní River drainage, Orinoco River basin, 5.01888, -61.11447, J.W. Armbruster, D.C. Werneke, T.P. Pera, N.K. Lujan, 12 June 2003.

Paratypes: AUM 36634, 2, 25.6-27.6 mm SL, Same information as holotype.

Diagnosis: Distinguished from *T. conradi*, *T. celsae*, and *T. ovidi* by spots present (vs. absent). Distinguished from *T. atoradorum*, *T. patamonorum*, *T. guianensis*, and *T. lewi* by pectoral-fin

ray count I,6 (vs. I,7–10). Distinguished from *T. martincarteri* and *T. cooperwiti* by having 38 vertebrae (vs. 37), 21 ventral procurrent rays (vs. 15–17), and 30 dorsal procurrent rays (vs. 21–22 and 26 respectively).

Description: Measurements and external meristics based on three specimens, internal meristics based on one cleared and stained specimen (see Tables 4 and 7). Species small, largest specimen 66.5 mm SL. Predorsal profile of body slightly convex dorsally and mostly flat ventrally, with dorsal portion flat in postdorsal region. Caudal peduncle tapers slightly posteriorly, then comes back to a concave point anteriorly, creating uppercase *W* with rounded bottom vertices, but procurrent caudal-fin rays remain flat with posterior profile of body giving entire caudal region rectangular appearance. Edges of caudal fin only slightly rounded before coming to corner, posterior edge truncate. Head trapezoidal from dorsal view and triangular from lateral view, compressing anteriorly in both views. Eyes dorsal, equidistant from anterior edge of premaxilla and nape, small and round. Subterminal mouth, nearly as wide as extent of anterior edge of head. Upper and lower lip joined by fleshy corner. Upper and lower lip with minute papillae. Upper lip extending into maxillary and rictal barbels just anterior to connection with bottom lip. Barbels all wider at base and narrow distally. Maxillary barbel slightly longer than nasal barbel, both much longer than rictal barbel. All barbels longer than snout length.

Pectoral fins with flat posterior edge and rounded on leading edge, with long filamentous extension of spine nearly doubling the length of the pectoral fin. Pectoral-fin rays I,6 (4). Pelvic fins longer than wide, leading edge curved, posterior edge also curved, originating anterior to dorsal fin insertion, slightly posterior to the middle of standard length (mean = 56%). Pelvic-fin rays I,4 (3) or I,3,I (1). Dorsal fin originating before posterior third of standard length (mean = 62.1%). Dorsal fin with three unbranched unsegmented rays in cleared and stained specimens

(iii, not visible in whole specimens): remaining dorsal-fin rays II,7 (4). Anal fin originating posterior to dorsal fin. Anal fin with three unbranched unsegmented rays in cleared and stained specimens (iii, not visible in whole specimens): remaining anal-fin rays II,5 (4). Caudal fin rays I,5 + 6,I (4). Anus slightly nearer to origin of anal fin than to origin of pelvic fins.

Interopercular odontode patch with 12–17 odontodes; opercular odontode patch with 9–18 odontodes. Vertebrae count 38, with 21 posterior to dorsal fin, 18 posterior to anal fin, and 11 posterior to anterior-most procurrent ray (1 cs). Dorsal procurrent rays 30; ventral procurrent rays 21 (1 cs). Parurohyal robust with large foramen, metapterygoid large and irregular, coming to a posterodorsal point and two dorsomedial points. Supraoccipital foramen long and thick, disconnected from teardrop-shaped anterior foramen pointed anteriorly. Sphenotic process directed anterolaterally. Pelvic girdle with two sharp anteromedial processes. Opercle thick. Posttemporo-supracleithrum with long anteromedially directed dorsal process. Dorsal ural process medium length and slender, with posterior process. Sharp process on ventral surface of ventral hypural.

Coloration: Cream colored ventrally gradually becoming light brown dorsally with darker brown patterning. Spotted throughout with large and small spots, all of which nearly perfectly circular. Largest spots follow the lateral line predorsally before dipping towards the posterior insertion of anal fin. Spots smaller towards head region. Dark stripe from eye to nasal barbel. Neurocranial region of head darker than rest of head.

Distribution: Known from only one locality in a tributary of the Yuruani River, a tributary to the Kukunan River of the Caroní river drainage in the Gran Sabana.

Etymology: Named for the Gran Sabana region, where this species is found.

***Trichomycterus martincarteri*, new species**

Holotype: To be designated.

Paratypes: All Collections Guyana, Cuyuní-Mazaruni (Region 7), Mazaruni River drainage, Essequibo River basin: ROM 83791, 5, 23.6-70.8 mm SL, Waruma Creek, Kako River, 5.4755, -60.77967, H. Lopez-Fernandez, D. C. Taphorn, E. A. Liverpool, C. Thierens, 20 April 2008; ROM 83818, 1, 70.7 mm SL, Waruma Creek - first set of rapids upstream from confluence with Kako river, Kako River, 5.49967, -60.77761, H. Lopez-Fernandez, D. C. Taphorn, E. A. Liverpool, C. Thierens, 22 April 2008; ROM 83833, 3, 40.2-68.9 mm SL, Paikwa River, Kako River, 5.48331, -60.73214, H. Lopez-Fernandez, D. C. Taphorn, E. A. Liverpool, C. Thierens, 22 April 2008; ROM 83834, 2, 57.6-59.7 mm SL, Paikwa River, Kako River, 5.48331, -60.73214, H. Lopez-Fernandez, D. C. Taphorn, E. A. Liverpool, C. Thierens, 22 April 2008; ROM 83842, 2, 65-75.6 mm SL, Paikwa River, Kako River, 5.48622, -60.73253, H. Lopez-Fernandez, D. C. Taphorn, E. A. Liverpool, Kramer K., 22 April 2008; ROM 89625, 1, 54.5 mm SL, Waruma Creek, Kako River, 5.381871, -60.720498, H. Lopez-Fernandez, D. C. Taphorn, E. A. Liverpool, S. Refvik, 11 March 2011; ROM 89627, 1, 40.4 mm SL, Waruma Creek, Kako River, 5.381871, -60.720498, H. Lopez-Fernandez, D. C. Taphorn, E. A. Liverpool, S. Refvik, 11 March 2011; ROM 89685, 1, 36.4 mm SL, Abbou Creek, 5.73623, -60.35956, H. Lopez-Fernandez, D. C. Taphorn, E. A. Liverpool, S. Refvik, 5 March 2011; ROM 89717, 2, 39.9-54.1 mm SL, Waruma Creek, Kako River, 5.381871, -60.720498, H. Lopez-Fernandez, D. C. Taphorn, E. A. Liverpool, S. Refvik, 11 March 2011; ROM 89725, 1, 46.7 mm SL, lower rapids of Abbou Creek, 5.73488, -60.36023, H. Lopez-Fernandez, D. C. Taphorn, E. A. Liverpool, J. Enright, 5 March 2011; ROM 93437, 2, 43.4-63.3 mm SL, Waruma Creek, Kako River, 5.475494682, -60.77899483, E. A. Liverpool, 6 November 2011; ROM 93441, 2, 55.2-61 mm SL, Waruma Creek, Kako River,

5.475494682, -60.77899483, E. A. Liverpool, 6 November 2011; ROM 93457, 1, 61.8 mm SL, Waruma Creek, Kako River, 5.47554892, -60.77899463, E. A. Liverpool, 6 November 2011; ROM 93469, 1, 42.9 mm SL, Waruma Creek, Kako River, 5.475693453, -60.77896704, E. A. Liverpool, 6 November 2011; ROM 93512, 1, 70.5 mm SL, Waruma Creek, Kako River, 5.486811111, -60.777675, E. A. Liverpool, 7 November 2011; ROM 93515, 4, 57.4-68.1 mm SL, Waruma Creek, Kako River, 5.486811111, -60.777675, E. A. Liverpool, 7 November 2011; ROM 93539, 1, 60.4 mm SL, Waruma Creek, Kako River, 5.486811111, -60.777675), E. A. Liverpool, 7 November 2011; ROM 93542, 1, 72.2 mm SL, Waruma Creek, Kako River, 5.486811111, -60.777675, E. A. Liverpool, 7 November 2011.

Diagnosis: Distinguished from *T. ovidi* by pectoral-fin ray count I,6–7 (vs. II,3–I,4). Distinguished from *T. atoradorum* and *T. cooperwiti*, by pectoral-fin ray count I,6–7 (vs. I,8–10). Distinguished from *T. gransabanensis*, and *T. guianensis* by vertebrae count 37 (vs. 38 and 39 respectively), 17 vertebrae posterior to anal fin (vs. 18 and 19 respectively), 16–17 vertebral procurrent rays (vs. 21 and 25 respectively), and 21–22 dorsal procurrent rays (vs. 30 and 39 respectively). Distinguished from *T. lewi* and *T. cooperwiti* by having 37 vertebrae (vs. 32–33). Distinguished from *T. celsae* by having 37 vertebrae (vs. 36). Distinguised from *T. patamornorum* by having 17 vertebrae posterior to the anal fin (vs. 18), by having 9–10 vertebrae posterior to the anterior-most procurrent ray (vs. 12), and by having 21–22 dorsal procurrent rays (vs. 26).

Description: Measurements and external meristics based on 33 specimens, internal meristics based on two cleared and stained specimens (see Tables 4 and 8). Species small, largest specimen 75.6 mm SL. Predorsal profile of body slightly convex dorsally and mostly flat ventrally, with dorsal portion flat in postdorsal region. Caudal peduncle tapers slightly

posteriorly, creating uppercase *U* with but procurrent caudal-fin rays remain flat with posterior profile of body giving entire caudal region rectangular appearance. Edges of caudal fin only slightly rounded before coming to corner, posterior edge truncate. Head trapezoidal from dorsal view and triangular from lateral view, compressing anteriorly in both views. Eyes dorsal, equidistant from anterior edge of premaxilla and nape, small and round. Subterminal mouth, nearly as wide as extent of anterior edge of head. Upper and lower lip joined by fleshy corner. Upper and lower lip with minute papillae. Upper lip extending into maxillary and rictal barbels just anterior to connection with bottom lip. Barbels all wider at base and narrow distally. Maxillary barbel very wide at base. Maxillary barbel equal to or slightly longer than nasal barbel, both much longer than rictal barbel. All barbels longer than snout length.

Pectoral fins with mostly flat posterior edge and rounded on leading edge, with long filamentous extension of spine nearly doubling the length of the pectoral fin. Pectoral-fin rays I,6 (30) or I,7 (3). Pelvic fins longer than wide, leading edge curved, posterior edge also nearly flat, originating anterior to dorsal fin insertion, slightly posterior to the middle of standard length (mean = 56%). Pelvic-fin rays I,4 (32) or II,3 (1). Dorsal fin originating near posterior third of standard length (mean = 64.1%). Dorsal fin with three unbranched unsegmented rays in cleared and stained specimens (iii, not visible in whole specimens): remaining dorsal-fin rays II,7 (31) or I,8 (2). Anal fin originating posterior to dorsal fin. Anal fin with three unbranched unsegmented rays in cleared and stained specimens (iii, not visible in whole specimens): remaining anal-fin rays II,5 (29), I,6 (3), or III,5 (1). Caudal fin rays I,5 + 6,I (30), I,4 + 6,I (1), I,6 + 5,I (1), or I,6 + 6,I (1). Anus equidistant from origin of anal fin and origin of pelvic fins.

Interopercular odontode patch with 16–35 odontodes; opercular odontode patch with 8–15 odontodes. Vertebrae count 37, with 21 posterior to dorsal fin, 17 posterior to anal fin, and 9–

10 posterior to anterior-most procurrent ray (2 cs). Dorsal procurrent rays 21–22; ventral procurrent rays 16–17 (2 cs). Parurohyal robust with large foramen, metapterygoid large and irregular, rounded on anterior and dorsomedial corners, with posteromedial notch, and sharp posterior corner. Supraoccipital foramen long, disconnected from large teardrop-shaped anterior foramen pointed anteriorly. Sphenotic process directed anterolaterally. Pelvic girdle with none or one anteromedial process. Opercle thick. Posttemporo-supracleithrum with anteromedially directed dorsal process. Dorsal ural process short.

Coloration: Coloration is on a spectrum of two forms, ranging from drab to spotted. Both forms cream colored ventrally gradually becoming light brown dorsally with darker brown patterning. Drab form appearing very plain in life, but slightly mottled by barely perceptible stippling on dorsal surface anterior to the dorsal fin in preserved specimens. More stippling perceptible on lateral portions of drab form in preserved specimens, especially towards the caudal fin. Spotted form with obvious dark brown stippling or almost perfectly circular spotting with very little variation in the sizes of the spots. Stipples or spots evenly distributed across lateral surface with no obvious patterning of the spots. Neurocranial portion of the head darker than the rest of the head.

Remarks: This species cannot always be easily distinguished by pattern. The drab gray-brown form is different than congeners, but this species displays a spotted form ranging from small stippling to small spots. When preserved, the stippled pattern becomes slightly more visible even on the drab individuals, especially in the caudal region. The stipples and spots on the spotted form appear more uniformly sized and shaped than the blotchier spotting of variable sizes on spotted congeners. The spotted form does not differ in measurements or meristics from the drab form. No osteological differences were noted between cleared and stained specimen of the drab

and spotted forms, with the exception of the presence of one anteromedial process on the pelvic girdle of the drab form (vs. no anteromedial processes on the pelvic girdle of the spotted form).

Distribution: Restricted to the Mazaruni River drainage, known from Waruma Creek and Paikwa Creek, which drain into the Kako River, a tributary to the Mazaruni River and from the Abbou Creek of the upper Mazaruni River drainage.

Etymology: Named in honor of Guyanese poet, revolutionist, and activist Matin Carter, writer of *Poems of Resistance from British Guiana*.

***Trichomycterus ovidi*, new species**

Holotype: Ex AUM 62949, 134.7 mm SL, Guyana; Potaro-Siparuni (Region 8), Moyow Creek upstream of Ayanganna Old, Potaro River drainage, Essequibo River basin, 5.304, -59.89819, D.C. Taphorn, E.A. Liverpool, D.C. Werneke, O. Williams, D.P. Fernandes, villagers, 20 March 2014.

Paratypes: AUM 62949, 11 (37.3–129.2 mm SL); Same information as holotype

Diagnosis: *Trichomycterus ovidi* is diagnosed from all *T. guianensis, T. ataradorum, T. patamonorum, T. cooperwiti, and T. gransabanensis* by spots absent (vs. present). It is additionally distinguished from all other Guiana Shield *Trichomycterus* by low fin ray counts, having II,5 dorsal-fin rays, I,4 pectoral-fin rays, II,1,I pelvic-fin rays, and II,4 anal-fin rays. It is distinguished from all *Trichomycterus* by having four pairs of ribs.

Description: Measurements and external meristics based on 12 specimens, internal meristics based on two cleared and stained specimens (see Tables 4 and 9). Species relatively large and elongate, largest specimen 134 mm SL. Predorsal profile of body long and mostly flat dorsally and mostly flat ventrally, with dorsal portion becoming convex as it reaches the head. Caudal

peduncle tapers posteriorly until truncation, but procurrent caudal-fin rays remain flat with the posterior profile of the body, giving the entire caudal region a rectangular appearance. Corners of caudal fin rounded. Caudal fin nearly flat on the posterior edge, but slightly convex. Head trapezoidal from dorsal view and triangular from lateral view, compressing anteriorly in both views. Eyes dorsal, closer to anterior edge of the premaxilla than nape, small and round. Subterminal mouth, nearly as wide as extent of anterior edge of head. Upper and lower lip joined by fleshy corner. Upper and lower lips with minute papillae. Upper lip extending into maxillary and rictal barbels just anterior to connection with the bottom lip. Barbels all wider at base and narrowing distally. Maxillary barbel very wide at base. Maxillary barbel longer than nasal barbel, and nasal barbel longer than rictal barbel. All barbels much longer than snout length.

Pectoral fins small with flat posterior edge joining rounded leading edge at an acute angle, with long filamentous extension of spine almost doubling length of fin. Pectoral-fin rays variable, but few in number, I,4,I (6), I,4 (4), or II,3,I (4). Pelvic fins minute, oval in shape, originating anterior to dorsal fin insertion, posterior middle of standard length (mean = 61.2%). Pelvic-fin rays variable, but total always total to four. Pelvic-fin rays IIII (7), II,1,I (5), or I,2,I (1). Dorsal fin originating at or past posterior third of standard length (mean = 67.8%). Dorsal fin with three unbranched unsegmented rays in cleared and stained specimens (iii, not visible in whole specimens); the remaining dorsal fin extremely variable in whole specimens: II,5,I (5), II,6,I (3), III,4,I (2), II,6 (1), III,5,I (1), or I,7 (1). Anal fin originating slightly posterior to dorsal fin. Anal fin with three unbranched unsegmented rays in cleared and stained specimens (iii, not visible in whole specimens): remaining anal-fin rays II,4,I (13) or III,4,I (1). Caudal fin rays I,5 + 6,I (12) or II,5+6,I (2). Anus much closer to origin of anal fin than origin of pelvic fins.

Interopercular odontode patch with 10–14 odontodes; opercular odontode patch with 12–16 odontodes. 50 vertebrae, with 22–23 posterior to dorsal fin, 19 posterior to anal fin, and 12–13 posterior to the anterior-most procurrent ray (2 cs). Dorsal procurrent rays 26; ventral procurrent rays 18–21 (2 cs). Parurohyal elongate, metapterygoid pointed dorsomedially and convex anteriorly. Supraoccipital foramen long with uniform width, disconnected from small circular anterior foramen. Sphenotic process directed anterolaterally. Pelvic girdle small. Posteroventral edge of opercle slightly sinusoidal. Posttemporo-supracleithrum with short and rounded anterodorsal process. Dorsal ural process short and thick. Small ventral ural process present. Four pairs of ribs.

Coloration: Pale yellow on the ventral surface, gradually becoming creamy and finally a dark brown on the dorsal surface. Pelvic and Anal fins pale. Leading edge of pectoral fin pale. Barbels lighter distally, rictal barbe pale. Opercular odontode patch pale.

Remarks: This is a unique form that is very interesting in that it inhabits habitat suitable for *Ituglanis* while appearing to possess a morphotype that is intermediate between *Trichomycterus* and *Ituglanis*, suggesting that *Trichomycterus* may be able to invade some lowland habitats and undergo speciation. It has been suggested that trichomycterines have potentially evolved lowland morphologies multiple times (Fernández *et al.*, 2021), and *T. ovidi* supports this idea. Multiple evolutions of lowland morphologies may complicate synapomorphic diagnoses of genera within Trichomycterinae.

Distribution: Known from one locality in Moyow Creek in the Potaro River drainage.

Etymology: Named in honor of Ovid Williams, who was the first indigenous pilot for the Guyana Defense Forces. Ovid has aided many researchers on trips to Guyana, including the

collection of *Trichomycterus ovidi*, by working with indigenous communities and serving as a font of knowledge about Guyana and its people.

***Trichomycterus patamonorum*, new species**

Holotype: To be designated.

Paratypes: Guyana, Potaro-Siparuni Region 8, Potaro River drainage, Essequibo River basin: AUM 62733, 13, 74.6–100.3 mm SL, Kuribrong River - mouth of Amaila River, 5.37608, -59.55053, D.C. Taphorn, E.A. Liverpool, Benjamin, 8 March 2014; AUM 62742, 1, 63.6 mm SL, Kuribrong River - just upstream of the mouth of Amila River, 5.37608, -59.55053, D.C. Taphorn, J.W. Armbruster, D.C. Werneke, E.A. Liverpool, D.P. Fernandes, 7 March 2014; AUM 62748, 10, 58.3–72.8 mm SL, Kuribrong River - right bank of third rapids, 5.33816, -59.56625, J.W. Armbruster, D.C. Taphorn, D.P. Fernandes, M. Benjamin, 8 March 2014; AUM 62754, 7, 54.4–94.2 mm SL, Kuribrong River - second rapids above Amaila Falls, 5.35081, -59.54483, J.W. Armbruster, D.C. Taphorn, D.P. Fernandes, M. Benjamin, 8 March 2014; AUM 62802, 10, 73.9–85.3 mm SL, Kuribrong River - first rapids above Amaila Falls, 5.37608, -59.55053, J.W. Armbruster, E.A. Liverpool, D.P. Fernandes, Pablo, Salvadore, 9 March 2014; AUM 62812, 3, 38–47.1 mm SL, Kuribrong River - riffle between first and second rapids above Amaila Falls, 5.36405, -59.54318, D.C. Taphorn, J.W. Armbruster, D.C. Werneke, E.A. Liverpool, D.P. Fernandes, M. Benjamin, 10 March 2014; AUM 62902, 14, 51.5–62.7 mm SL, Kiwiparu Crrek Grass Falls Creek near top of falls, Kuribrong River, 5.40532, -59.5439, D.C. Taphorn, J.W. Armbruster, D.C. Werneke, E.A. Liverpool, 14 March 2014; ROM 91352, 18, 55.7–88 mm SL, Guyana, Unnamed East bank tributary at 4th rapid, Kuribrong River, 5.314144364, -59.55153276, N. K. Lujan, D. Abraham, D. Stoby, D. Gordon, Benji, S. Lythcutt, 23 October

2011; ROM 91493, 1, 74 mm SL, Kuribrong River at upstream-most rapid, 5.275417732, -59.70121778, N. K. Lujan, D. Abraham, D. Stoby, D. Gordon, O. Williams, 25 October 2011; ROM 94991, 2, 44.8–59.6 mm SL, Itabu Creek, Kuribrong River, 5.29113, -59.71923, D. C. Taphorn, E. A. Liverpool, H. Lopez-Fernandez, M. Benjamin, G. Pablo, 28 March 2014. **Nontypes:** Guyana, Potaro-Siparuni Region 8, Potaro River drainage, Essequibo River basin: AUM 28148, 4, 60.8–97.9 mm SL, Chenapou Cataract, 5.00139, -59.62583, L.M. Page, J.W. Armbruster, M. Hardman, J.H. Knouft, W.S. Prince, 31 October 1998; AUM 45167, 1, 83.4 mm SL, Rapids upstream of Wachima Creek, Chenapou Creek, 4.9668, -59.58103, L.S. de Souza, N.K. Lujan, D.C. Taphorn, J.A. Hartsell, E. Liverpool, S. Lord, 11 December 2005; AUM 45399, 9, 37.3–101.9 mm SL, Chenapou River rapids 1 mile upstream from mouth of creek, 4.96667, -59.85103, L.S. de Souza, N.K. Lujan, D.C. Taphorn, J.A. Hartsell, E. Liverpool, S. Lord, 10 December 2005; AUM 62910, 9, 35.3–100.5 mm SL, Potaro River at Ayanganna Old, Essequibo River basin, 5.30181, -59.89838, D.C. Taphorn, D.C. Werneke, E.A. Liverpool, D.P. Fernandes, 16 March 2014; AUM 62935, 1, 34.1 mm SL, Potaro River at western side of Ayanganna Old, Essequibo River basin, 5.30181, -59.89838, D.C. Taphorn, D.C. Werneke, E.A. Liverpool, D.P. Fernandes, 19 March 2014; INHS 49567, 3, 68.1–101.7 mm SL, Chenapou Cataract, 5.001389, -59.62583, L.M. Page, J.W. Armbruster, M. Hardman, J.H. Knouft & W.S. Prince, 31 October 1998; ROM 89932, 6, 64.3–93.5 mm SL, Kopanang River at schoolhouse rapids at the Village landing, 4.95407, -59.85882, N. K. Lujan, T. F. Teixera, March 2011; ROM 89940, 2, 30.5–50.5 mm SL, Yarbro Creek, Kopanang River, 4.94252, -59.82533, T. F. Teixera, P. Moses, 29 March 2011; ROM 95000, 2, 36.8–38.5 mm SL, Potaro River, Essequibo River basin, 5.005816667, -59.63028333, H. Lopez-Fernandez, M. Kolmann, Danny, Denise, Mark, Wenceslaus, 16 March 2014; ROM 95076, 1, 31.6 mm SL, Potaro River, Essequibo River basin,

5.06263, -59.66042, H. Lopez-Fernandez, M. Kolmann, Danny, Denise, Mark, Wenceslaus, 21 March 2014. GUYANA, Cuyuni-Mazaruni Region 7, Mazaruni River drainage, Essequibo River basin: AUM 35585, 5, 30–53.7 mm SL, Orokang River near Chi-Chi Falls airstrip, 5.52519, -60.23224, J.W. Armbruster, M.H. Sabaj, D.C. Werneke, C.L. Allison, M.R. Thomas, C.J. Chin, D. Arjoon, 13 November 2002; AUM 35590, 5, 29.8–51.7 mm SL, Orokang River at Chi-Chi Falls airstrip, 5.5349, -60.23318, J.W. Armbruster, M.H. Sabaj, D.C. Werneke, C.L. Allison, M.R. Thomas, C.J. Chin, D. Arjoon, 13 November 2002; ROM 83790, 6, 39.8–74.3 mm SL, Waruma Creek, Kako River, 5.4755, -60.77967, H. Lopez-Fernandez, D. C. Taphorn, E. A. Liverpool, C. Thierens, K. Kramer, 20 April 2008; ROM 83804, 2, 51.6–79.3 mm SL, Waruma Creek, Kako River, 5.48606, -60.78956, H. Lopez-Fernandez, D. C. Taphorn, E. A. Liverpool, C. Thierens, 21 April 2008; ROM 89590, 1, 54.4 mm SL, Waruma Creek, Kako River, 5.4755, -60.776667, H. Lopez-Fernandez, D. C. Taphorn, E. A. Liverpool, S. Refvik, 11 March 2011; ROM 89618, 1, 62.6 mm SL, Waruma Creek, Kako River, 5.381871, -60.720498, E. A. Liverpool, D. C. Taphorn, S. Refvik, G. Kramer, 11 March 2011; ROM 89696, 1, 50.7 mm SL, Sanda Creek area above Wishek Falls, Kako River, 5.58132, -60.80864, H. Lopez-Fernandez, D. C. Taphorn, E. A. Liverpool, S. Refvik, 9 March 2011; ROM 89716, 1, 56.1 mm SL, Waruma Creek, Kako River, 5.381871, -60.720498, H. Lopez-Fernandez, D. C. Taphorn, E. A. Liverpool, S. Refvik, 11 March 2011.; ROM 93441, 6, 44–59 mm SL, Waruma Creek, Kako River, 5.475494682, -60.77899483, E. A. Liverpool, 6 November 2011; ROM 93451, 3, 40–50.7 mm SL, Waruma Creek, Kako River, 5.47554892, -60.77899463, E. A. Liverpool, 6 November 2011; ROM 93459, 1, 44.7 mm SL, Waruma Creek, Kako River, 5.475693453, -60.77896704, E. A. Liverpool, 6 November 2011; ROM 93482, 1, 50.4 mm SL, Waruma Creek, Kako River, 5.46978421, -60.77971052, E. A. Liverpool, 7 November 2011; ROM 93511, 1, 72.9 mm SL,

Waruma Creek, Kako River, 5.486811111, -60.777675, E. A. Liverpool, 7 November 2011; ROM 93526, 1, 38 mm SL, Waruma Creek, Kako River, 5.486811111, -60.777675, E. A. Liverpool, 7 November 2011; ROM 93539, 4, 50.4–67.5 mm SL, Waruma Creek, Kako River, 5.486811111, -60.777675, E. A. Liverpool, 7 November 2011.

Venezuela, Bolivar State, Caroni River drainage, Orinoco River basin: AUM 36615, 6, 34.9-79 mm SL, Mereman Paru River, tributary to Apanwao River, 5.74335, -61.40337, J.W. Armbruster, D.C. Werneke, T.P. Pera, N.K. Lujan, 11 June 2003; AUM 36653, 1, 36.5 mm SL, Ikabaru River, 4.41422, -61.71755, J.W. Armbruster, D.C. Werneke, O Leon, N.K. Lujan, 13 June 2003; AUM 36680, 5, 26.4-32.8 mm SL, Chirima River, tributary to Yuruani River, tributary to Kukunan River, 5.03499, -60.97288, J.W. Armbruster, D.C. Werneke, T.P. Pera, N.K. Lujan, 15 June 2003; AUM 36681, 12, 22.2-54.1 mm SL, Chirima River, tributary to Yuruani River, tributary to Kukunan River, 5.03499, -60.97288, J.W. Armbruster, D.C. Werneke, T.P. Pera, N.K. Lujan, 15 June 2003.

Diagnosis: Distinguished from *T. conradi*, *T. celsae*, and *T. ovidi* by patterned spots (vs. no pattern). Distinguished from *T. guianensis*. *T. martincarteri*, *T. cooperwiti*, and *T. gransabanensis* by having I,8–10 pectoral-fin rays (vs. I,6–7). Distinguished from *T. atoradorum* by pattern and having 33–34 vertebrae (vs. 36), and 10–11 ventral procurrent rays (vs. 14). Distinguished from *T. lewi* by having 33–34 vertebrae (vs. 35) and narrowed supraoccipital foramen.

Description: Measurements and external meristics based on 177 specimens, internal meristics based on eight cleared and stained specimens (see Tables 4 and 10). Species small, largest specimen 101.9 mm SL. Predorsal profile of body convex dorsally and mostly flat ventrally, with dorsal portion flattening out in postdorsal region. Caudal peduncle bevels slightly at origin of

caudal-fin rays, but procurrent caudal-fin rays remain flat with posterior profile of body, giving entire caudal region parallel appearance. Corners of caudal fin only round slightly before coming to point, posterior edge concave, caudal fin emarginate to lunate. Head trapezoidal from dorsal view and triangular from lateral view, compressing anteriorly in both views. Eyes dorsal, equidistant from nape and anterior edge of premaxilla, small and round. Subterminal mouth, nearly as wide as extent of anterior edge of head. Upper and lower lip joined by fleshy corner. Upper and lower lip with minute papillae. Upper lip extending into maxillary and rictal barbels just anterior to connection with bottom lip. Barbels all wider at base and narrowing distally. Nasal barbel slightly longer than maxillary barbel, both much longer than rictal barbel. Nasal and maxillary barbels longer than snout length. Rictal barbel shorter than snout length.

Pectoral fins with flat posterior edge and rounded on leading edge, with long filamentous extension of spine roughly half as long as spine length. Pectoral-fin rays usually I,9 (119), I,8 (57), or very rarely I,7 (3) or I,10 (1). Pelvic fins longer than wide, leading edge curved, posterior edge also curved, oval in appearance, originating anterior to dorsal fin insertion, almost at middle of standard length (mean = 54.5%). Pelvic-fin rays I,4 (179). Dorsal fin originating before posterior third of standard length (mean = 61.2%). Dorsal fin with two or three unbranched unsegmented rays in cleared and stained specimens (ii-iii, not visible in whole specimens): remaining dorsal-fin rays II,7 (167), III,6 (5), III,7 (2), II,6 (3), or II,8 (2). Anal fin originating posterior to dorsal fin. Anal fin with three unbranched unsegmented rays in cleared and stained specimens (iii, not visible in whole specimens): remaining anal-fin rays II,5 (169), I,6 (4), III,5 (2), II,6 (2), II,4 (1), or III,4 (1). Caudal fin rays I,5 + 6,I (183) and very rarely I,5+5,2 (2). Anus slightly closer to origin of anal fin than origin of pelvic fins.

Interopercular odontode patch with 12–82 odontodes; opercular odontode patch with 4–14 odontodes. Vertebrae count 33–34, with 19–21 posterior to dorsal fin, 15–16 posterior to anal fin, and 5–7 posterior to anterior-most procurrent ray (7 cs). Dorsal procurrent rays 12–14; ventral procurrent rays 10–11 (8 cs). Parurohyal short, metapterygoid rhomboidal, coming to posterodorsal point and dorsomedial point. Supraoccipital foramen always narrowed anteriorly, sometimes closed off entirely creating another small foramen, always disconnected from small anteriorly pointed anterior foramen. Sphenotic process directed anterolaterally. Pelvic girdle slender, with one or two sharp anteromedial processes. Posteroventral edge of opercle nearly straight. Posttemporo-supracleithrum with sharp anterodorsal process. Dorsal ural process short but slender. Small, wide ventral protuberance on ventral hypural.

Coloration: Cream-colored ventrally gradually becoming creamy light brown dorsally with dark brown patterning. Patterns comprised of blotchy maculae, relatively uniform maculae, and uniformly circular spotting that is lighter than maculae. Patterns extremely variable. Usually somewhat regular horizontally stretched oval maculae following lateral line. When both blotchy maculae and smaller uniformly circle spotting occur, spotting seems to be inferior to maculae. Spotting can also occur on fin rays, while blotches seemingly do not invade fins. Maculae often form almost uniformly horizontal rows above, below, and on lateral line. These maculae tend to run together horizontally on smaller individuals, never forming solid lines, but sometimes creating dashed or dot dashed patterns, especially row following lateral line. Posterior neurocranial region of head darker than rest of head.

Remarks: *Trichomycterus patamonorum* is apparently the most abundant species of the Pakaraima mountains and has a much larger range than any other species described in this thesis. Additionally, it overlaps in distribution with at least six other *Trichomycterus*.

The type locality was restricted to the Kuribrong River. Given that the loricariid catfish *Corymbophanes* has different species in the upper Kuribrong and upper Potaro (Lujan et al., 2019), the type locality was restricted in case future studies found differences among the populations. There seems to be some genetic structuring between the Mazaruni and Potaro populations, but the branch lengths are short. There are no available tissues or sequences of the Caroní populations. From the measurements and meristics taken here, the pectoral-fin rays do not clearly separate the populations, but provide some interesting trends. The Kuribrong (Potaro) population has almost entirely I,9 pectoral-fin rays, while the mainstem Potaro populations have a more even mix of individuals with I,8 and I,9 pectoral-fin rays, the Mazaruni populations has more individuals with I,8 than I,9 pectoral-fin rays, and the Caroní populations never have I,9 pectoral-fin rays, having almost always I,8 and very rarely I,7 in very small individuals. This suggests fairly recent movement from the Mazaruni to the Caroni and Potaro drainages.

Distribution: Ranges throughout many headwaters of the Caroní, Potaro and Mazaruni Rivers. Known from the Mazaruni, Potaro, Chenapau, Orokang, Kuribrong, Kopanang, Kako, Apanwao, and Yuruani rivers.

Etymology: *Patamonorum* is the Latin plural neuter genitive of Patamona. It is named for the indigenous people who live in the native range of this species.

Discussion

Trichomycterus is a paraphyletic genus due to a lack of synapomorphies within its separate lineages (de Pinna, 1998). This lack of clear synapomorphies tends to trickle down within clades, making it difficult to find clear morphologic features between species. This can be seen within the handful of previously described members of the *T. guianensis* clade. Nalbant and Lineras (1987) synonymized *T. conradi* with *T. guianense* due to a lack of obvious morphological difference, which was admitted in the original description of these two species (Eigenmann, 1912). Reexamination of the type material almost 20 years after these two species were synonymized provided a morphologic basis for the separation of these as two distinct species (DoNascimiento & Villareal, 2005) - a result reinforced here by caudal peduncle length and depth, postdorsal length, and barbel lengths (supplementary Table 1). Of the 11 species examined in this study, two are easily identifiable by pattern and general morphology. *Trichomycterus ovidi* n. sp. is very elongate and not distinctly patterned, gradually whitish-yellow from the ventral side to a darker brown dorsally, with the dorsal and anal fins very far posterior on the body, and reduced pelvic fins. *Trichomycterus atoradorum* n. sp. has a pattern dominated by a mostly solid horizontal stripe originating from the opercular odontodes and following the lateral line through the medial caudal fin rays. Of the remaining nine species, *T. celsae, T. c.f. celsae*, and *T. conradi* are a group of plainly patterned fishes, and *T. guianensis, T. cooperwiti* n. sp., *T. patamonoroum* n. sp., *T. gransabanensis* n. sp., and *T. lewi* have spots. *Trichomycterus martincarteri* n. sp. displays a variety of patterning from plain with barely perceptible stippled spots, to stippled spots, to large spots, and thus has to be distinguished from both groups. Less conspicuous external morphologies (i.e. measurements and meristics) were sufficient to distinguish most other species (see diagnoses in taxonomic accounts), however

osteology was necessary to distinguish between *T. cooperwiti* n. sp. and *T. guianensis*. My recovery of many unique morphologies with several species being known from only one or a few headwater streams suggests that there are likely many other species of *Trichomycterus* in the Pakaraima Mountains, and the distinct form of *T. atoradorum* n. sp. from Kusad Mountain suggests the potential for unique *Trichomycterus* in the neighboring Kanuku mountains, which would have drained into the proto-Berbice and have not been extensively sampled. Only Moco Moco creek (Takutu drainage) has been sampled for fishes, and no *Trichomycterus* were collected (JWA pers. comm.)

Two species examined here (*T. ovidi* n. sp. and *T. c.f. celsae*) are of great interest because they appear to have apomorphies of both *Trichomycterus* and *Ituglanis*. *Ituglanis* is diagnosed by a reduced or absent supraoccipital foramen (vs. large), an anteriorly directed sphenotic process (vs. antero-lateral or lateral), a half-circle metapterygoid (vs. pointed or any other shape), an elongate parurohyal (vs. robust), fewer ribs (typically fewer than 8 in *Ituglanis* vs. usually more than 10 in *Trichomycterus*) and a concave medial margin of the autopalatine (vs. almost straight) (Costa & Bockmann, 1993; Costa *et al.*, 2021). However as more species are described, some traits are being reconsidered. For example, the formerly diagnostic autopalatine is now considered ambiguous (Costa *et al.*, 2021), and the robustness of the parurohyal may not be phylogenetically informative (Datovo & Bockmann, 2010). *Trichomycterus ovidi* n. sp. displays the *Trichomycterus* characters for the supraoccipital foramen, metapterygoid (pointed) and sphenotic, but the *Ituglanis* character for the autopalatine, number of ribs (four pairs), and elongate parurohyal. *Trichomycterus ovidi* n. sp. is firmly in the *T. guianensis* clade in phylogenetic analyses, therefore the number of ribs is likely convergent, and may be related to the sluggish habitat preference that is more similar to the preference of *Ituglanis* (Hayes *et al.*,

2020). *Trichomycterus ovidi* n. sp. is the first Trichomycterine outside of *Ituglanis* to be recorded with four pairs of ribs (see Costa *et al.*, 2021). The autopalatine and parurohyal of *T. ovidi* n. sp. add support to these traits not being diagnosable for *Ituglanis* (see Datovo & Bockmann, 2010; Costa *et al.*, 2021). *Trichomycterus c.f. celsae* displays the *Trichomycterus* characters for the sphenotic, autopalatine, metapterygoid (trapezoidal), and paurohyal, but the *Ituglanis* character for the supraoccipital foramen. There is currently no cleared and stained specimen for *T. c.f. celsae*, so I was unable to count the number of ribs. *Trichomycterus cachiraensis* and *Cambeva brachykeknos* also have a reduced supraoccipital foramen which Costa *et al.* (2021) suggested represent independent acquisitions. Molecular data will be needed to confirm the placement of *T. c.f. celsae* in the Trichomycteridae.

All four gene trees recovered reciprocal monophyly for all species except for *T. conradi*. The low support for the *T. conradi* from the Potaro River as sister to the *T. conradi* from the Ireng River in the *16S* tree and unresolved relationship in the *rag2* tree is likely due to the relatively low number of total disagreements in the alignments of these two genes compared to *COI* and *cytb*. Because of this, any number of differences between populations will represent relatively large amounts of divergence. The reciprocal monophyly recovered by the *COI* tree provides support to the conclusion of Reis and De Pinna (2022) that *COI* may be helpful to identify different species of *Trichomycterus*, however, this should be used as a supplementary tool alongside morphological evidence.

Because of poor support for the deeper nodes in the concatenated dataset, I cannot make conclusions of relationships outside of the focal *Trichomycterus guianensis* clade. The support values for deeper nodes were similar to that of Ochoa *et al.* (2017), and did not recover the topology proposed by Ochoa *et al.* (2020). This reinforces the notion that TSS of only a handful

of loci is not enough data to draw conclusions for clade relationships within the Trichomycterinae. For the remainder of the discussion, I follow the hypothesized topology from Ochoa *et al.* (2020) for relationships outside of the focal *T. guianensis* clade.

My phylogenetic results recovered two subclades within the *Trichomycterus guianensis* clade. Based on the specimens examined here, there does not appear to be any clear synapomorphies that would separate these clades. The *T. ovidi/cooperwiti/guianensis* subclade does appear to have more post-anal vertebrae, post-procurrent vertebrae, and dorsal procurrent rays, suggesting that the anal fin originates slightly more anterior on the body and that the procurrent rays span a longer section of the caudal region. The *T. patamonorum/martincarteri/atoradorum* subclade tends to have more interopercular odontodes on average. However, these traits may all be unrelated to phylogenetic signal. As more species are discovered and included in these subclades, a more thorough revision of their osteology should be considered. *Trichomycterus conradi* was recovered in different topologies based on the concatenated analysis with MrBayes and time-calibrated analysis with BEAST, trading positions with *T. atoradorum* n. sp. However, *T. conradi* is recovered as a monophyletic wide-ranging, proto-Berbice endemic found below the Pakaraima plateau. The topological discordance of this species between my analyses is likely unresolved due to a lack of taxonomic coverage of other *Trichomycterus* from the proto-Berbice. Genetic samples are lacking from *Trichomycterus* from Venezuela.

My estimates of divergence are roughly 5-10 million years younger than the estimates made by Ochoa *et al.* (2017) and Costa *et al.* (2022), but the estimates made in those papers are well within the highest probability distributions (HPDs) reported here. It must be clearly pointed out that my divergence estimates have extremely wide HPDs. Ochoa *et al.* (2017) did not report

HPDs, and Costa *et al.* (2022) used a much stronger prior for their secondary time calibration than should be used, potentially resulting in narrower HPDs. The prior used by Costa *et al.* (2022) was based on an age estimated by Betancur-R *et al.* (2015) by using mean nodal ages of a Bayesian tree produced by Betancur-R *et al.* (2013) as secondary calibration points. The HPDs of nodes nearby the Trichomycteridae (e.g. the Callicthyidae-Nematogenyidae node) span 30-40 million years in the original time-calibration (Betancur-R *et al.*, 2013), therefore the prior distribution should certainly be much larger than the roughly six million years of space that was sampled by the model implemented by Costa *et al.* (2022). The HPDs reported in the present study are wide, and estimates recovered from molecular time-calibrations have a low degree of precision.

There are three viable options to increase the precision of our time-calibrations within the Trichomycteridae. One option is to increase the precision of the prior distribution of a secondary calibration point of the origin of the Siluriformes, which can be done by increasing sampling quality and quantity extant bony fishes and/or by accurately placing more fish fossils distributed across all time periods into a time-calibrated phylogeny. Progress is being made on that front (see Betancur-R *et al.*, 2013; Betancur-R *et al.*, 2017). However, that would still require the implementation of a secondary calibration, when primary calibrations are preferred (Schenk, 2016). The other two remaining options would allow researchers to use a primary calibration with a FBD model. The FBD model is currently the best practice for time calibrating a phylogeny because it estimates the divergence time and branch lengths using the same tree model, instead of estimating branch lengths under the tree model, and then estimating a divergence date based on a most recent common ancestor prior (Heath *et al.*, 2014). Because the fossilized birth-death process is driven by four interacting parameters, a strong prior on only one

parameter will increase the precision of the posteriors. Increased fossil representation and increased taxonomic representation would both provide stronger priors that would increase the precision of FBD models. There are many difficulties in recovering fossils let alone being able to assign those fossils to a specific group (Parham *et al.*, 2012). Better taxonomic sampling in a FBD model would certainly increase precision of the model (Barido-Sottani *et al.*, 2018), but that will also require a massive revision of Trichomycteridae.

My results support the claim by Ochoa *et al.* (2017) that the *T. guianensis* clade likely diverged prior to the uplift of the northern Andes. Additionally, I recover the oldest common ancestor of the *Eremophilus* lineage at 18.48 Ma. This time period in South America is geologically busy, following the Incaic phase and diverging during the Quecha phase of the Andean Orogeny, setting the stage for the modern river drainages of South America (Albert *et al.*, 2018). At this time, the major rivers of Guyana were much different, with the Proto-Berbice skirting the southern edge of the Pakaraima Mountains, en route to the modern day Berbice River (Lujan & Armbruster, 2011). At the same time, the Potaro and Mazaruni may have flown North into the Cuyuní River, as evidenced by these modern rivers spilling Eastwards over Precambrian outcrops instead of being restrained to a valley, flowing away from an area of Rupununi Surface that has been uplifted 150-250 feet since the end of the Tertiary (McConnell, 1968). The proto-Berbice may have allowed the expansion of *Trichomycterus* into the Pakaraima Mountains, where the *T. guianensis* clade then diversified. From there, headwater captures or wet season flooding connections may have provided access through the Pakaraima Mountains and into the Mazaruni and Cuyuní Rivers (see Figure 8 for hypothesized routes of these paleo-rivers). The recovery of *T. atoradorum* n. sp. with *T. patamonorum* n. sp. and *T. martincarteri* n. sp. would indicate that the same common ancestor that invaded the Mazaruni River also invaded Kusad

Mountain, a distinct mountain separated from the rest of the Pakaraimas by the Takutu graben as well as the Pakaraima Mountains, suggesting that the proto-Berbice path to the Pakaraimas is likely. However, more sampling will be needed to piece together this puzzle.

Ochoa *et al.* (2020) recovered strong support for *Eremophilus mutisii* (along with a couple other *Trichomycterus* from the Magdalena River) as sister to the rest of the *Eremophilus* lineage. As mentioned previously, the age estimate of this lineage coincides with the gradual uplift of the Andes. Additionally, *E. mutisii* is an air-breathing, lowland species (Cala, 1987), suggesting that the common ancestor for this lineage was a lowland species, an ecotype still seen in *Ituglanis*. *Eremophilus mutisii* is native to the Magdelena River drainage. The uplift of the Northern Andes separating the Magdelena River from the rest of the South American lowlands may have preserved this lowland species while the remaining lowland forms were subject to be impacted by habitat changes caused by the formation of the modern Amazon and by marine incursions. These drastic habitat changes may have allowed for the modern diversification of *Ituglanis*.

The molecular monophyly of *Trichomycterus patamonorum* n. sp. across the Mazaruni, Potaro, and Kuribrong suggests that there may be modern connectivity between the headwaters of the Mazaruni and Potaro rivers. Anecdotal reports of connections in excessively wet seasons and the presence of suitable fissures between headwaters is little more to stake this claim on (Hayes *et al.*, 2020), but more collections should be made in these headwaters to validate or refute this claim. Molecular samples from the Venezuela population of *T. patamonorum* will also be necessary to assess the genetic connectedness of this species across its entire range. There is some apparent structuring between the Mazaruni and Potaro drainages, but the branch lengths are small. These populations may be in the early stages of speciation, or connections may still be

made intermittently, such as during historical floods that may only occur every 10-100 years. Additionally, the close relationship of *T. patamonorum* n. sp. with *T. martincarteri* n. sp. supports the hypothesis of McConnell (1968) that, during the time of the Proto-Berbice, the Potaro River joined the Mazaruni River and flowed North into the Cuyuní River. Additionally, the interdigitization of the upper Ireng and Potaro Rivers (Lujan & Armbruster, 2011) taken into consideration with the relationship of *T. cooperwiti* n.sp. with *T. guianensis* and *T. ovidi* n. sp. as well as a similar Ireng and Potaro River sister relationship between *Corymbophanes* and *Yalowak* (Lujan *et al.*, 2020) suggests that the upper Ireng may have flowed into the Potaro-Mazaruni-Cuyuní (hereafter the Grand Pakaraima River) while the middle and lower Ireng River would have flowed south into the Proto-Berbice (Figure 8) (see Nascimento *et al.*, 2019). More exploration of the Pakaraima Mountains is needed to examine the drainage limits of both the Proto-Berbice and Grand Pakaraima River, as well as to search for potential connections between the two paleo-drainages. The *Trichomycterus* of the Guiana Shield are found in high elevation headwaters with few other fishes, and many of these upland tributaries have yet to be sampled. The Trichomycterids yet to be discovered will help tell the complex biogeographical story of the ancient Pakaraima Mountains.

References

Albert, J. S., P. Val & C. Hoorn. 2018. The changing course of the Amazon River in the Neogene: center stage for Neotropical diversification. Neotropical Ichthyology, 16. Available at http://www.scielo.br/j/ni/a/Y8BqkSjr3TVDjQnHhdWMDzx/abstract/?lang=en [Accessed 20 June 2022].

Armbruster, J. W. 2011. Global catfish biodiversity. Pp. 15–37 In: American Fisheries Society Symposium.

Arratia F., G., A. Chang G., S. M. Marque & G. Rojas M. 1978. About Bullockia gen. nov., Trichomycterus mendozensis n. sp. and revision of the family Trichomycteridae (Pisces, Siluriformes). Studies on Neotropical Fauna and Environment, 13: 157–194.

Arratia, G. 1998. Silvinichthys, a new genus of trichomycterid catfishes from the Argentinian Andes, with redescription of Trichomycterus nigricans. Ichthyological Exploration of Freshwaters, 9: 347–370.

Barido-Sottani, J., V. Bošková, L. D. Plessis, D. Kühnert, C. Magnus, V. Mitov, N. F. Müller, J. PečErska, D. A. Rasmussen, C. Zhang, A. J. Drummond, T. A. Heath, O. G. Pybus, T. G. Vaughan & T. Stadler. 2018. Taming the BEAST—A Community Teaching Material Resource for BEAST 2. Systematic Biology, 67: 170–174.

Baskin, J. N. 1973. Structure and relationships of the Trichomycteridae. City University of New York.

Baskin, J. N., T. M. Zaret & F. Mago-Leccia. 1980. Feeding of Reportedly Parasitic Catfishes (Trichomycteridae and Cetopsidae) in the Rio Portuguesa Basin, Venezuela. Biotropica, 12: 182–186.

Bell, M. A. & G. T. Lloyd. 2015. strap: an R package for plotting phylogenies against stratigraphy and assessing their stratigraphic congruence. Palaeontology, 58: 379–389.

Betancur-R, R., R. E. Broughton, E. O. Wiley, K. Carpenter, J. A. López, C. Li, N. I. Holcroft, D. Arcila, M. Sanciangco, J. C. Cureton Ii, F. Zhang, T. Buser, M. A. Campbell, J. A. Ballesteros, A. Roa-Varon, S. Willis, W. C. Borden, T. Rowley, P. C. Reneau, D. J. Hough, G. Lu, T. Grande, G. Arratia & G. Ortí. 2013. The tree of life and a new classification of bony fishes. PLoS currents, 5: ecurrents.tol.53ba26640df0ccaee75bb165c8c26288.

Betancur-R, R., G. Ortí & R. A. Pyron. 2015. Fossil-based comparative analyses reveal ancient marine ancestry erased by extinction in ray-finned fishes. Ecology Letters, 18: 441–450.

Betancur-R, R., E. O. Wiley, G. Arratia, A. Acero, N. Bailly, M. Miya, G. Lecointre & G. Ortí. 2017. Phylogenetic classification of bony fishes. BMC Evolutionary Biology, 17: 162.

Bogan, S. & F. L. Agnolin. 2009. Primer registro fósil de la familia Trichomycteridae (Teleostei: Siluriformes; Plioceno) en la Formación Monte Hermoso, Argentina. Revista del Museo Argentino de Ciencias Naturales, 11: 193–198.

Bouckaert, R., J. Heled, D. Kühnert, T. Vaughan, C.-H. Wu, D. Xie, M. A. Suchard, A. Rambaut & A. J. Drummond. 2014. BEAST 2: A Software Platform for Bayesian Evolutionary Analysis. PLOS Computational Biology, 10: e1003537.

Bouckaert, R. R. & A. J. Drummond. 2017. bModelTest: Bayesian phylogenetic site model averaging and model comparison. BMC Evolutionary Biology, 17: 42.

Cala, P. 1987. Aerial respiration in the catfish, Eremophilus mutisii (Trichomycteridae, Siluriformes), in the Rio Bogota Basin, Colombia. Journal of Fish Biology, 31: 301–303.

Costa, W. J. E. M. 2021. Comparative Osteology, Phylogeny and Classification of the Eastern South American Catfish Genus Trichomycterus (Siluriformes: Trichomycteridae). Taxonomy, 1: 160–191.

Costa, W. J. E. M. & F. A. Bockmann. 1993. Un nouveau genre néotropical de la famille des Trichomycteridae (Siluriformes: Loricarioidei). Un nouveau genre néotropical de la famille des Trichomycteridae (Siluriformes: Loricarioidei), 20: 43–46.

Costa, W. J. E. M., A. M. Katz, J. L. O. Mattos, P. F. Amorim, B. O. Mesquita, P. J. Vilardo & M. A. Barbosa. 2019. Historical review and redescription of three poorly known species of the catfish genus Trichomycterus from south-eastern Brazil (Siluriformes: Trichomycteridae). Journal of Natural History, 53: 2905–2928.

Costa, W. J. E. M., J. L. O. Mattos & A. M. Katz. 2021. Phylogenetic Position of Trichomycterus payaya and Examination of Osteological Characters Diagnosing the Neotropical Catfish Genus Ituglanis (Siluriformes: Trichomycteridae). Zoological Studies, 60: e43.

Costa, W. J. E. M., J. L. O. Mattos, W. M. S. Sampaio, P. Giongo, F. B. de Almeida & A. M. Katz. 2022. Phylogenetic relationships of a new catfish of the genus Trichomycterus (Siluriformes, Trichomycteridae) from the Brazilian Cerrado, and the role of Cenozoic events in the diversification of mountain catfishes. Zoosystematics and Evolution, 98: 151–164.

Datovo, A. & F. A. Bockmann. 2010. Dorsolateral head muscles of the catfish families Nematogenyidae and Trichomycteridae (Siluriformes: Loricarioidei): comparative anatomy and phylogenetic analysis. Neotropical Ichthyology, 8: 193–246.

De Queiroz, K. 2007. Species Concepts and Species Delimitation. Systematic Biology, 56: 879–886.

DoNascimiento, C. & O. Villareal. 2005. Estatus taxonómico y sistemático de la población de bagres tricomictéridos de la cueva del Guácharo (Otophysi, Siluriformes). Pp. 44–50 In: Memorias del VIII Simposio Colombiano de Ictiología. Quibdó, Colombia.

Eigenmann, C. H. 1909. The Fresh-water Fishes of Patagonia and an Examination of the Archiplata-Archhelonis Theory.

Eigenmann, C. H. 1912. The Freshwater Fishes of British Guiana, Including a Study of the Ecological Grouping of Species and the Relation of the Fauna of the Plateau to that of the Lowlands. Carnegie Institute.

Eigenmann, C. H. 1917. Descriptions of Sixteen New Species of Pygidiidæ. Proceedings of the American Philosophical Society, 56: 690–703.

Eigenmann, C. H. 1918. The Pygidiidae, a family of South American catfishes.

Fernández, L. 2017. Family Trichomycteridae - Pencil Catfishes, Torrent Catfishes, and Parasitic Catfishes (Candirus). Pp. 311–322 In: Field Guide to the Fishes of the Amazon, Orinoco, and Guianas. Princeton University Press

Fernández, L., J. Arroyave & S. A. Schaefer. 2021. Emerging patterns in phylogenetic studies of trichomycterid catfishes (Teleostei, Siluriformes) and the contribution of Andean diversity. Zoologica Scripta, 50: 318–336.

Fricke, R., W. N. Eschmeyer & J. D. Fong. 2022. Eschmeyer's Catalog of Fishes - Genera/Species by Family/Subfamily. Available at https://researcharchive.calacademy.org/research/ichthyology/catalog/SpeciesByFamily.asp [Accessed 20 June 2022].

Gill, T. 1872. Arrangement of the Families of Fishes Or Classes Pisces, Marsipobranchii, and Leptocardii Prepared for the Smithsonian Institution by Theodore Gill. Smithsonian Institution.

Hayes, M. M., H. J. Paz, C. C. Stout, D. C. Werneke & J. W. Armbruster. 2020. A hotspot atop: rivers of the Guyana Highlands hold high diversity of endemic pencil catfish (Teleostei: Ostariophysi: Siluriformes). Biological Journal of the Linnean Society, 129: 862–874.

Heath, T. A., J. P. Huelsenbeck & T. Stadler. 2014. The fossilized birth–death process for coherent calibration of divergence-time estimates. Proceedings of the National Academy of Sciences, 111: E2957–E2966.

Hubert, N. & J.-F. Renno. 2006. Historical biogeography of South American freshwater fishes. Journal of Biogeography, 33: 1414–1436.

Huelsenbeck, J. P. & F. Ronquist. 2005. Bayesian Analysis of Molecular Evolution Using MrBayes. Pp. 183–226 In: Nielsen, R. (ed.). Statistical Methods in Molecular Evolution. Statistics for Biology and Health. New York, NY, Springer Available at https://doi.org/10.1007/0-387-27733-1_7 [Accessed 24 June 2022].

von Humboldt, A. 1805. Mémoire sur l'Eremophilus et Astroblepus, deux nouveaux genres de l'ordre des apodes. Voyage de Humboldt et Bonpland, Deuxième partie. Observations de Zoologie et d'Anatomie compare. Paris: F. Schell, G. Dufour et Companie, : 17–20.

Katoh, K., K. Misawa, K. Kuma & T. Miyata. 2002. MAFFT: a novel method for rapid multiple sequence alignment based on fast Fourier transform. Nucleic Acids Research, 30: 3059–3066.

Katz, A. M., M. A. Barbosa, J. L. de O. Mattos & W. J. E. M. da Costa. 2018. Multigene analysis of the catfish genus Trichomycterus and description of a new South American trichomycterine genus (Siluriformes, Trichomycteridae). Zoosystematics and Evolution, 94: 557–566.

Kearse, M., R. Moir, A. Wilson, S. Stones-Havas, M. Cheung, S. Sturrock, S. Buxton, A. Cooper, S. Markowitz, C. Duran, T. Thierer, B. Ashton, P. Meintjes & A. Drummond. 2012. Geneious Basic: An integrated and extendable desktop software platform for the organization and analysis of sequence data. Bioinformatics, 28: 1647–1649.

Kelley, W. E. & J. W. Atz. 1964. A Pygidiid Catfish That Can Suck Blood from Goldfish. Copeia, 1964: 702–704.

Lasso, C. A. & F. Provenzano. 2002. Dos nuevas especies de bagres del género Trichomycterus (Siluriformes: Trichomycteridae) de la Gran Sabana, Escudo de las Guayanas, Venezuela. Revista de Biología Tropical, 50: 1139–1149.

Lovejoy, N. R. & B. B. Collette. 2001. Phylogenetic Relationships of New World Needlefishes (Teleostei: Belonidae) and the Biogeography of Transitions between Marine and Freshwater Habitats. Copeia, 2001: 324–338.

Lujan, N. K. & J. W. Armbruster. 2011. The Guiana Shield. Pp. 224 In: Historical biogeography of Neotropical freshwater fishes. University of California Press Berkeley

Lujan, N. K., J. W. Armbruster, D. C. Werneke, T. F. Teixeira & N. R. Lovejoy. 2020. Phylogeny and biogeography of the Brazilian–Guiana Shield endemic Corymbophanes clade of armoured catfishes (Loricariidae). Zoological Journal of the Linnean Society, 188: 1213–1235.

Lundberg, J. G., L. G. Marshall & J. Guerrero. 1998. The stage for Neotropical fish diversification: a history of tropical South American rivers. In: Malabara, L. R., R. E. Reis, R. P. Vari, Z. M. S. Lucena & C. A. S. Lucena (eds.). Phylogeny and Classification of Neotropical Fishes. Edipucrs

Machado, F. A. & I. Sazima. 1983. Comportamento alimentar do peixe hematófago Branchioica bertonii (Siluriformes, Trichomycteridae). Ciência e Cultura, 35: 343–348.

Mayden, R. L. 1997. A hierarchy of species concepts: the denouement in the saga of the species problem.

McConnell, R. B. 1968. Planation Surfaces in Guyana. The Geographical Journal, 134: 506–520.

Miles, C. 1943. On three recently described species and a new genus of pygidiid fishes from Colombia. Revista de la Academia Colombiana de Ciencias Exactas, Fisicas y Naturales, 5: 367–369.

Miller, E. C. & C. Román-Palacios. 2021. Evolutionary time best explains the latitudinal diversity gradient of living freshwater fish diversity. Global Ecology and Biogeography, 30: 749–763.

Miller, E. & C. Román-Palacios. Evolutionary time explains the global distribution of freshwater fish diversity.

Miller, M. & W. Pfeiffer. 2010. Schwartz Terri. Creating the CIPRES Science Gateway for inference of large phylogenetic trees. Pp. 1–8 In: Proceedings of the Gateway Computing Environments Workshop. New Orleans, LA.

Montaña, C. G., E. Liverpool, D. C. Taphorn & C. M. Schalk. 2021. The cost of gold: Mercury contamination of fishes in a Neotropical river food web. Neotropical Ichthyology, 19. Available at http://www.scielo.br/j/ni/a/4j8bxhg9thqs5DMN8H4R4jh/abstract/?lang=en [Accessed 8 December 2021].

Nalbant, T. & O. Linares. 1987. A study of a subterranean population of Trichomycterus guianense (Eigenmann, 1909) from Venezuela (Pisces, Siluriformes, Trichomycteridae).

Nascimento, F. A., A. A. Gomes, A. A. R. Salgado & S. S. Tavares Júnior. 2019. Evidências de rearranjo de drenagem na Bacia do Alto rio Branco, Amazónia. In: Atas do IX Congresso Nacional de Geomorfologia: Gomorfologia 2019: Que futuro para a geomorfologia...?

Ochoa, L. E., A. Datovo, C. DoNascimiento, F. F. Roxo, M. H. Sabaj, J. Chang, B. F. Melo, G. S. C. Silva, F. Foresti, M. Alfaro & C. Oliveira. 2020. Phylogenomic analysis of trichomycterid catfishes (Teleostei: Siluriformes) inferred from ultraconserved elements. Scientific Reports, 10: 2697.

Ochoa, L. E., F. F. Roxo, C. DoNascimiento, M. H. Sabaj, A. Datovo, M. Alfaro & C. Oliveira. 2017. Multilocus analysis of the catfish family Trichomycteridae (Teleostei: Ostariophysi: Siluriformes) supporting a monophyletic Trichomycterinae. Molecular Phylogenetics and Evolution, 115: 71–81.

Oliveira, C., G. S. Avelino, K. T. Abe, T. C. Mariguela, R. C. Benine, G. Ortí, R. Vari & R. Corrêa e Castro. 2011. Phylogenetic relationships within the speciose family Characidae (Teleostei: Ostariophysi: Characiformes) based on multilocus analysis and extensive ingroup sampling. BMC Evolutionary Biology, 11: 275.

Palumbi, S. R. & C. S. Baker. 1994. Contrasting population structure from nuclear intron sequences and mtDNA of humpback whales. Molecular Biology and Evolution, 11: 426–435.

Panelli, L. F. 2019. Is Guyana a new oil El Dorado? The Journal of World Energy Law & Business, 12: 365–368.

Parham, J. F., P. C. J. Donoghue, C. J. Bell, T. D. Calway, J. J. Head, P. A. Holroyd, J. G. Inoue, R. B. Irmis, W. G. Joyce, D. T. Ksepka, J. S. L. Patané, N. D. Smith, J. E. Tarver, M. van Tuinen, Z. Yang, K. D. Angielczyk, J. M. Greenwood, C. A. Hipsley, L. Jacobs, P. J. Makovicky, J. Müller, K. T. Smith, J. M. Theodor, R. C. M. Warnock & M. J. Benton. 2012. Best Practices for Justifying Fossil Calibrations. Systematic Biology, 61: 346–359.

de Pinna, M. C. C. 1989. A new sarcoglanidine catfish, phylogeny of its subfamily, and an appraisal of the phyletic status of the Trichomycterinae (Teleostei, Trichomycteridae). American Museum novitates;; no. 2950.

de Pinna, M. C. C. 1992. A new subfamily of Trichomycteridae (Teleostei, Siluriformes), lower loricarioid relationships and a discussion on the impact of additional taxa for phylogenetic analysis. Zoological Journal of the Linnean Society, 106: 175–229.

de Pinna, M. C. C. 2016. The dawn of phylogenetic research on Neotropical fishes: a commentary and introduction to Baskin (1973), with an overview of past progress on trichomycterid phylogenetics. Neotropical Ichthyology, 14. Available at http://www.scielo.br/scielo.php?script=sci_arttext&pid=S1679-62252016000200219&lng=en&tlng=en [Accessed 20 June 2022].

de Pinna, M. de. 1998. Phylogenetic relationships of neotropical Siluriformes: Historical overview and synthesis of hypotesis. Pp. 279–330 In: Malabara, L. R., R. E. Reis, R. P. Vari, Z. M. S. Lucena & C. A. S. Lucena (eds.). Phylogeny and Classification of Neotropical Fishes. Edipucrs

de Queiroz, K. 2005. Ernst Mayr and the modern concept of species. Proceedings of the National Academy of Sciences, 102: 6600–6607.

R Core Team. 2022. R: A Language and Environment for Statistical Computing. Vienna, Austria. Available at https://www.r-project.org/ [Accessed 23 June 2022].

Rambaut, A., A. J. Drummond, D. Xie, G. Baele & M. A. Suchard. 2018. Posterior Summarization in Bayesian Phylogenetics Using Tracer 1.7. Systematic Biology, 67: 901–904.

Reis, V. & M. De Pinna. 2022. Diversity and systematics of Trichomycterus Valenciennes 1832 (Siluriformes: Trichomycteridae) in the Rio Doce Basin: iterating DNA, phylogeny and classical taxonomy. Zoological Journal of the Linnean Society, : zlac018.

Schenk, J. J. 2016. Consequences of Secondary Calibrations on Divergence Time Estimates. PLOS ONE, 11: e0148228.

Souza, L. S. de, J. W. Armbruster & D. C. Werneke. 2012. The influence of the Rupununi portal on distribution of freshwater fish in the Rupununi district, Guyana/L'influence du portail du Rupununi sur la distribution des poissons dulcaquicoles dans le district du Rupununi, Guyana. Cybium, International Journal of Ichthyology, 36: 31–44.

de Souza, L. S., J. W. Armbruster & P. W. Willink. 2020. Connectivity of Neotropical River Basins in the Central Guiana Shield Based on Fish Distributions. Frontiers in Forests and Global Change, 3. Available at https://www.frontiersin.org/article/10.3389/ffgc.2020.00008 [Accessed 21 June 2022].

Stadler, T. 2009. On incomplete sampling under birth–death models and connections to the sampling-based coalescent. Journal of Theoretical Biology, 261: 58–66.

Stankowski, S. & M. Ravinet. 2021. Quantifying the use of species concepts. Current Biology, 31: R428–R429.

Suchard, M. A., P. Lemey, G. Baele, D. L. Ayres, A. J. Drummond & A. Rambaut. 2018. Bayesian phylogenetic and phylodynamic data integration using BEAST 1.10. Virus Evolution, 4: vey016.

Taylor, W. R. & G. Van Dyke. 1985. Revised procedures for staining and clearing small fishes and other vertebrates for bone and cartilage study. Cybium (Paris), 9: 107–119.

Tchernavin, V. V. 1944. A Revision of some Trichomycterinæ based on material preserved in the British Museum (Natural History). Proceedings of the Zoological Society of London, 114: 234–275.

Tomassini, R. L., C. I. Montalvo, C. M. Deschamps & T. Manera. 2013. Biostratigraphy and biochronology of the Monte Hermoso Formation (early Pliocene) at its type locality, Buenos Aires Province, Argentina. Journal of South American Earth Sciences, 48: 31–42.

Valenciennes, A. 1832. Nouvelles observations sur le Capitan de Bogota, Eremophilus mutisii. In: Recueil d'observations de zoologie et d'anatomie comparée: faites dans l'Océan Atlantique, dans l'interieur du nouveau continent et dans la Mer du Sud, pendant les années 1799, 1800, 1801, 1802 et 1803. F. Schoell et G. Dufour

Villa-Verde, L., H. Lazzarotto & S. M. Lima. 2012. A new glanapterygine catfish of the genus Listrura (Siluriformes: Trichomycteridae) from southeastern Brazil, corroborated by morphological and molecular data. Neotropical Ichthyology, 10: 527–538.

Ward, R. D., T. S. Zemlak, B. H. Innes, P. R. Last & P. D. N. Hebert. 2005. DNA barcoding Australia's fish species. Philosophical Transactions of the Royal Society B: Biological Sciences, 360: 1847–1857.

Wheeler, Q. D. & R. Meier. 2000. Species Concepts and Phylogenetic Theory: A Debate. Columbia University Press.

Winemiller, K. O., H. López-Fernández, D. C. Taphorn, L. G. Nico & A. B. Duque. 2008. Fish assemblages of the Casiquiare River, a corridor and zoogeographical filter for dispersal between the Orinoco and Amazon basins. Journal of Biogeography, 35: 1551–1563.

Winemiller, K. O., P. B. McIntyre, L. Castello, E. Fluet-Chouinard, T. Giarrizzo, S. Nam, I. G. Baird, W. Darwall, N. K. Lujan, I. Harrison, M. L. J. Stiassny, R. a. M. Silvano, D. B. Fitzgerald, F. M. Pelicice, A. A. Agostinho, L. C. Gomes, J. S. Albert, E. Baran, M. Petrere, C. Zarfl, M. Mulligan, J. P. Sullivan, C. C. Arantes, L. M. Sousa, A. A. Koning, D. J. Hoeinghaus, M. Sabaj, J. G. Lundberg, J. Armbruster, M. L. Thieme, P. Petry, J. Zuanon, G. T. Vilara, J. Snoeks, C. Ou, W. Rainboth, C. S. Pavanelli, A. Akama, A. van Soesbergen & L. Sáenz. 2016. Balancing hydropower and biodiversity in the Amazon, Congo, and Mekong. Science, 351: 128–129.

Winemiller, K. O. & H. Y. Yan. 1989. Obligate Mucus-Feeding in a South American Trichomycterid Catfish (Pisces: Ostariophysi). Copeia, 1989: 511–514.

Figures and Tables

Figure 1: Schematics of measurements taken. A:anal, D: dorsal, Dia: diameter, Dp: Depth, Hd: head, HL: head length, L: length, Ped: peduncle, SL: standard length.

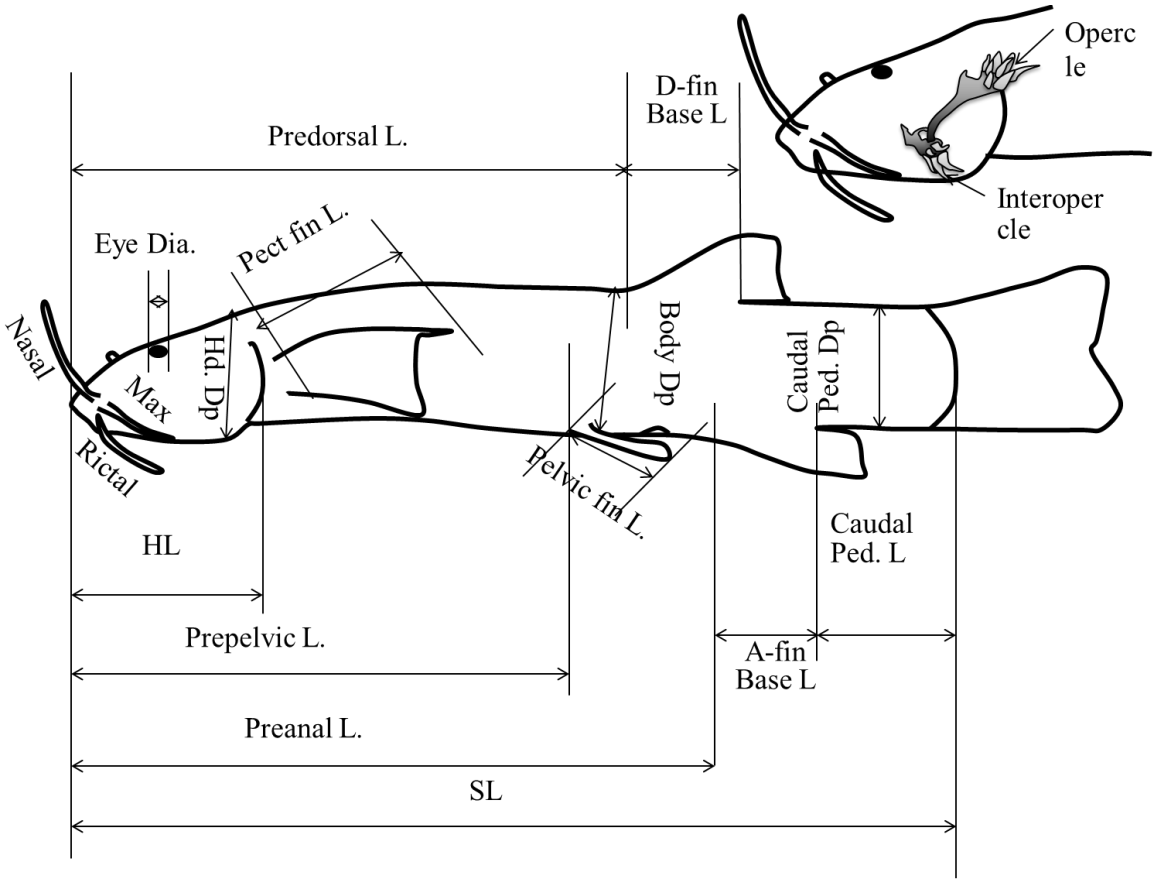

Figure 2: The number of vertebrae interacting with the procurrents include the vertebra with the neural/hemal spine anterior to the most anterior procurrent to and including the hypural and the number of vertebrae posterior to the anal and dorsal fins include the vertebrae with the neural/hemal spine directly anterior to the most anterior pterygiophore.

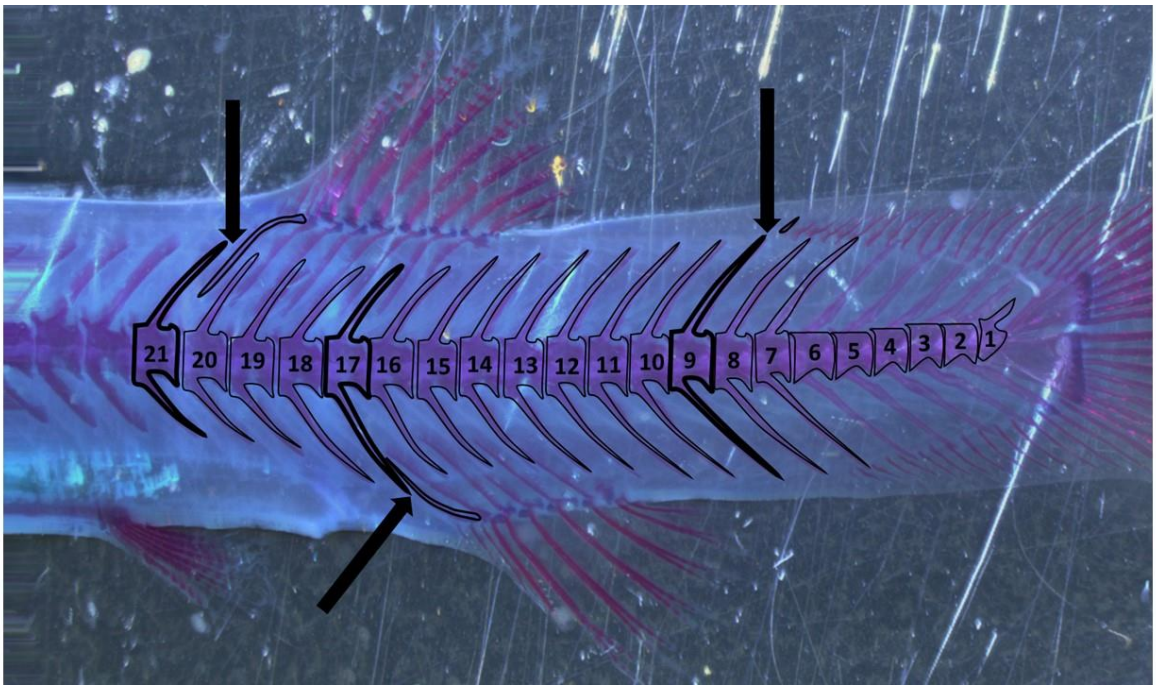

Figure 3: Osteological characters examined: Dorsolateral view of neurocranium (A), ventral view of pelvic girdle (B), and lateral view of ural plate (C).

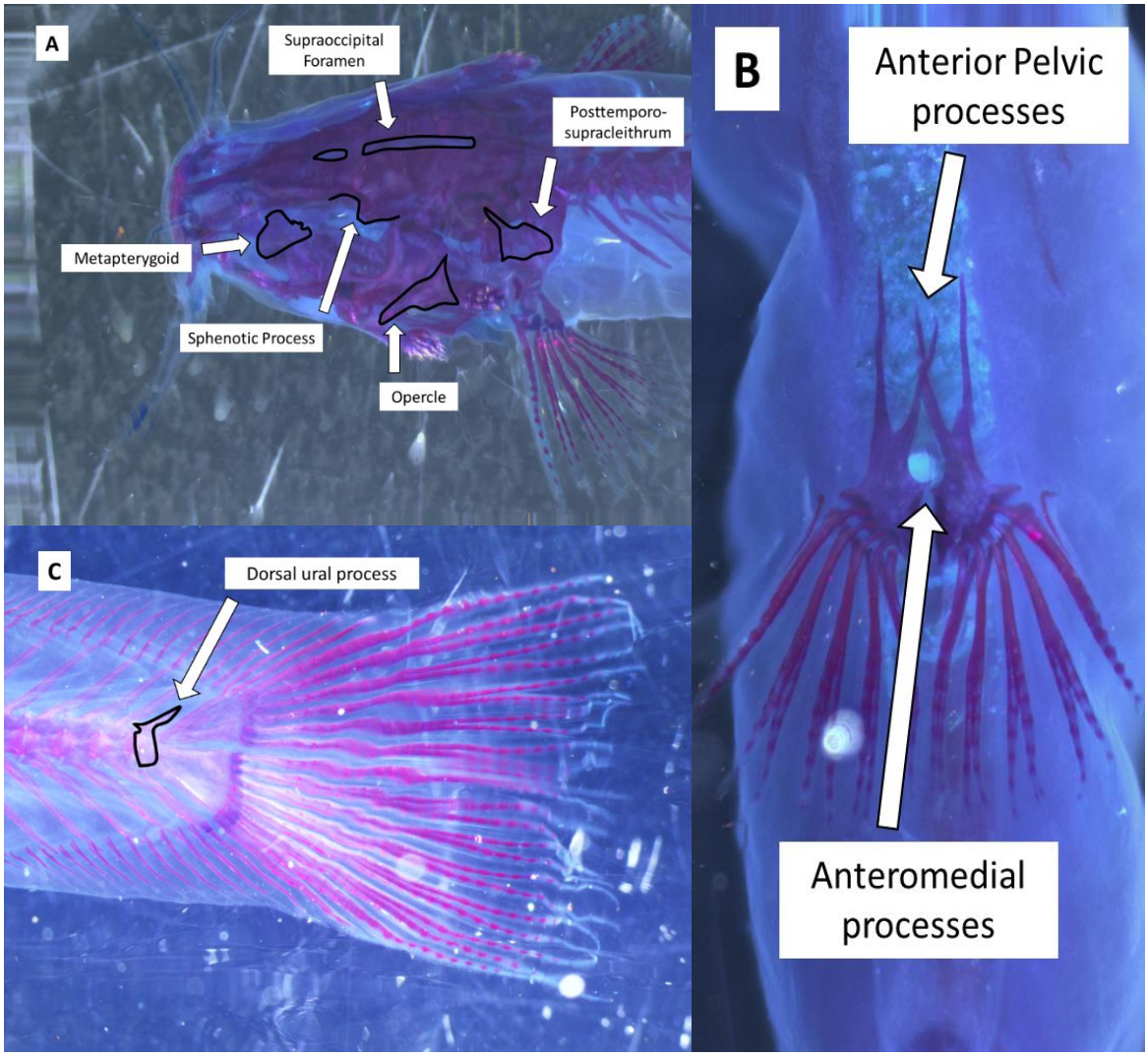

Figure 4: Gene trees for A) *16S*, B) *COI*, C) *cytB*, and D) *rag2*. Red circles represent posterior probabilities less than 75, gray circles represent posterior probabilities from 75-95, and black circles represent posterior probabilities greater than 95

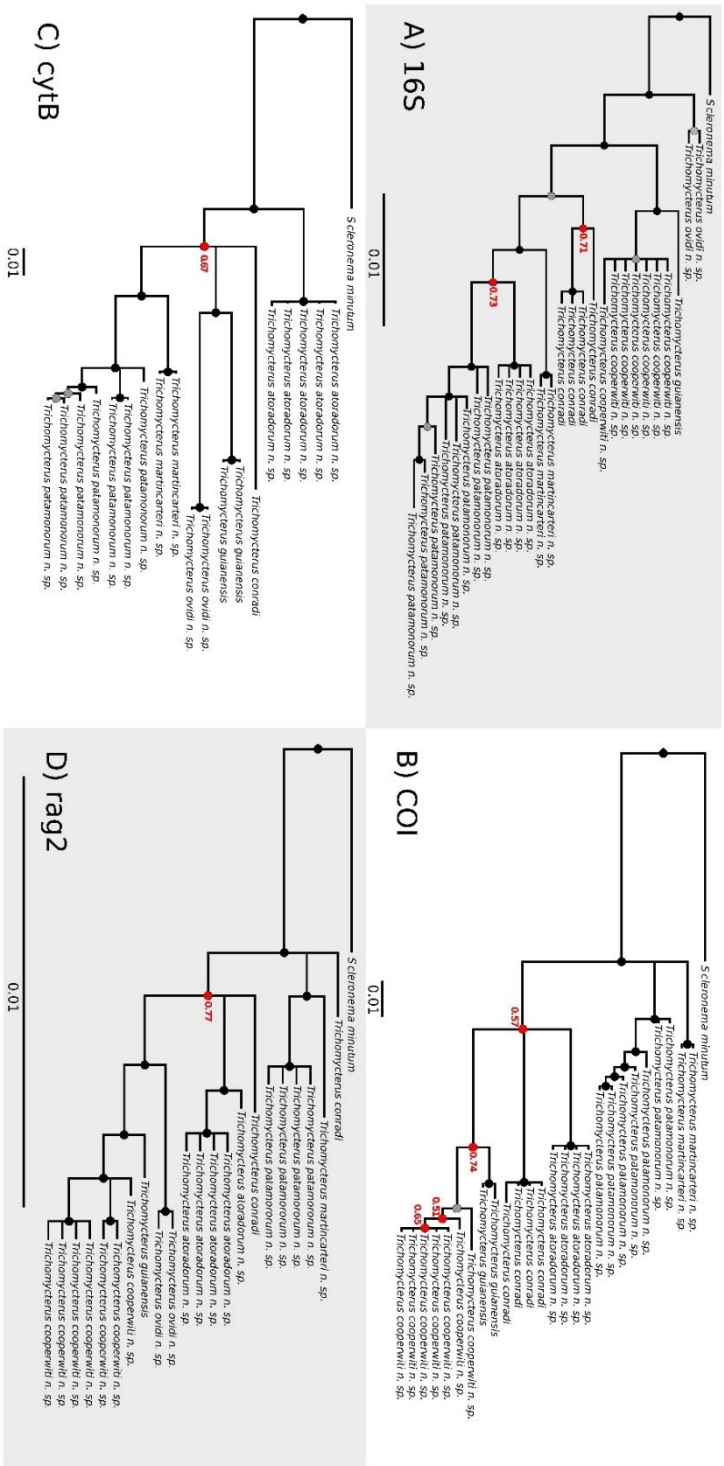

Figure 5: Concatenated BI Tree. Collapsed clades are consistent with the lineages, subfamilies, genera, and clades hypothesized by Ochoa *et al.* (2020). Red circles represent posterior probabilities less than 75, gray circles represent posterior probabilities from 75-95, and black circles represent posterior probabilities greater than 95

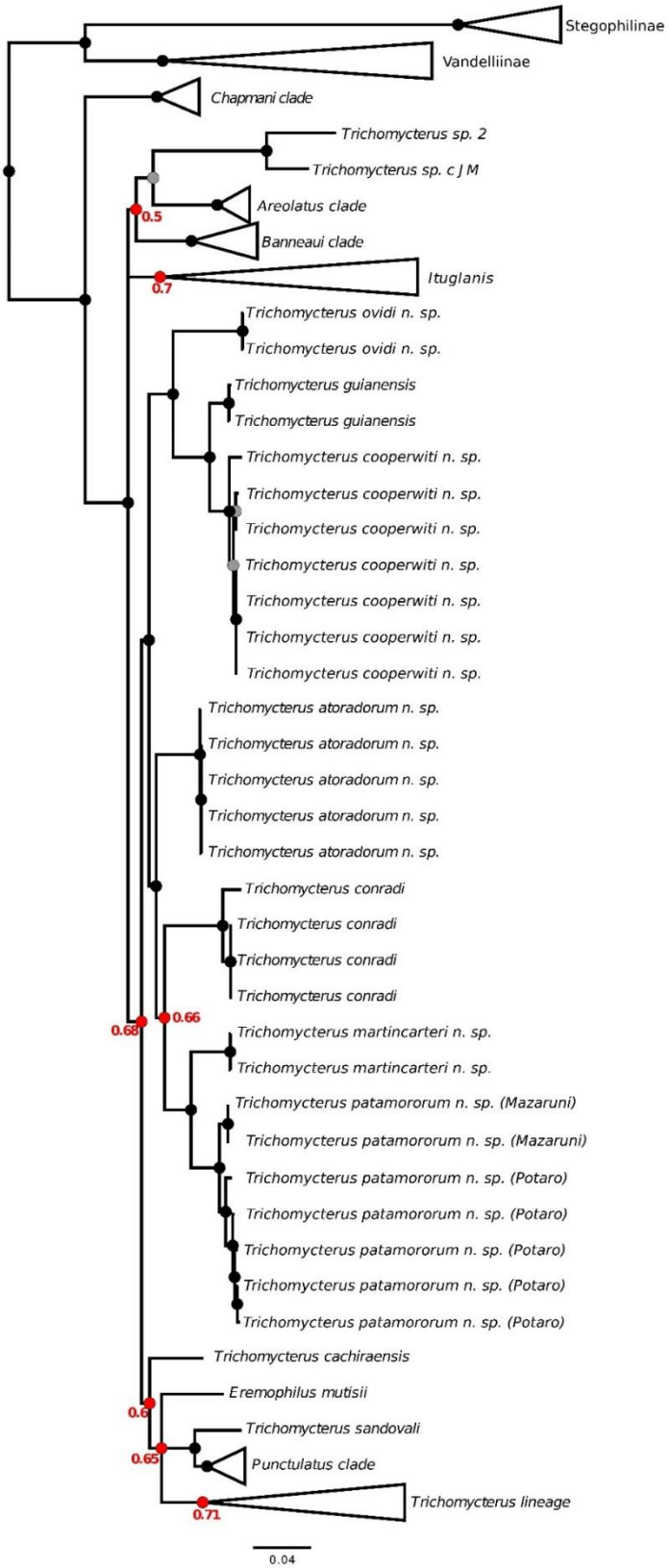

Figure 6: Time-calibrated tree of the *Eremophilus* lineage. Red circles represent posterior probabilities less than 75, gray circles represent posterior probabilities from 75-95, and black circles represent posterior probabilities greater than 95; 95% HPDs represented by blue bars, and the red bar represents the 95% HPD for the most recent common ancestor to the *Eremophilus* lineage.

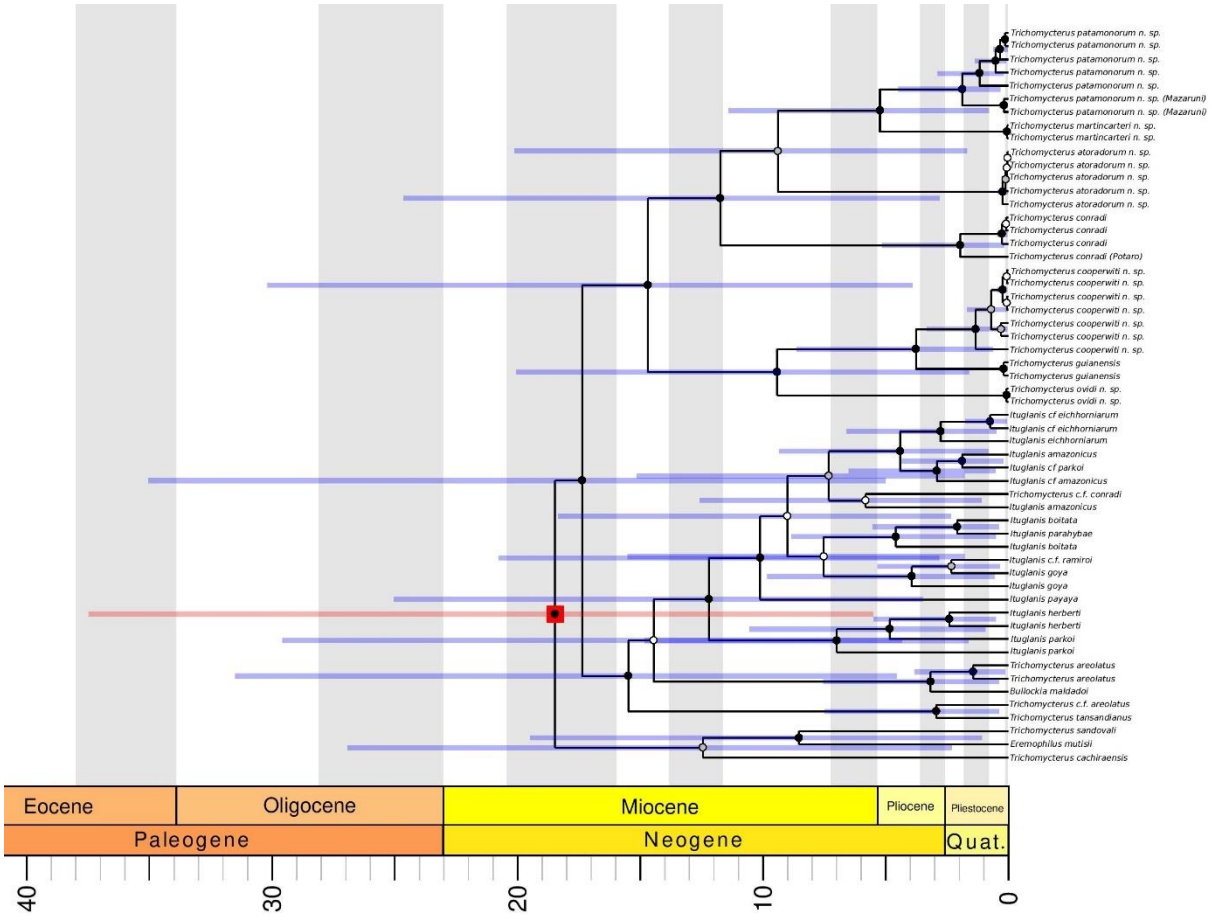

Figure 7: Localities of comparative materials and new species of Guiana Shield *Trichomycterus*.

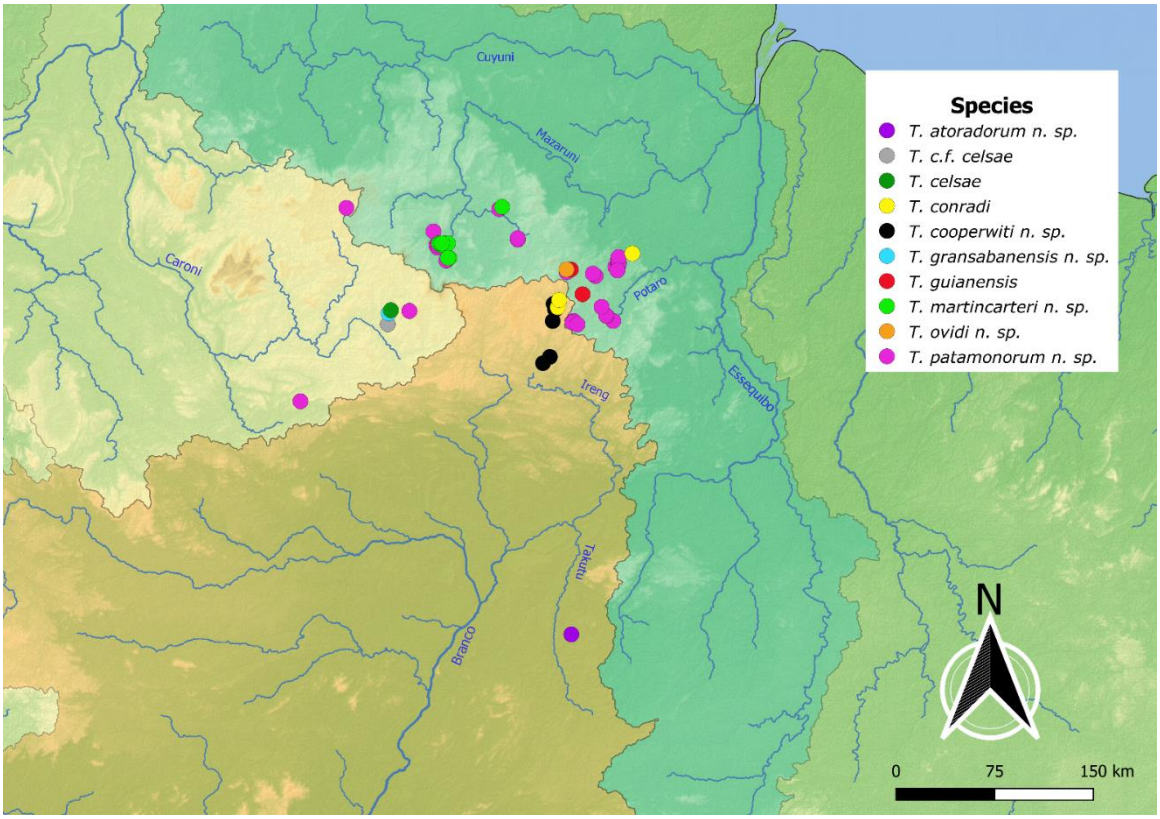

Figure 8: Map of Rio Branco, Essiquibo, and Caroní River drainages with hypothesized routes of the Proto-Berbice (long dashes) and Grand Pakaraima River (short dashes)

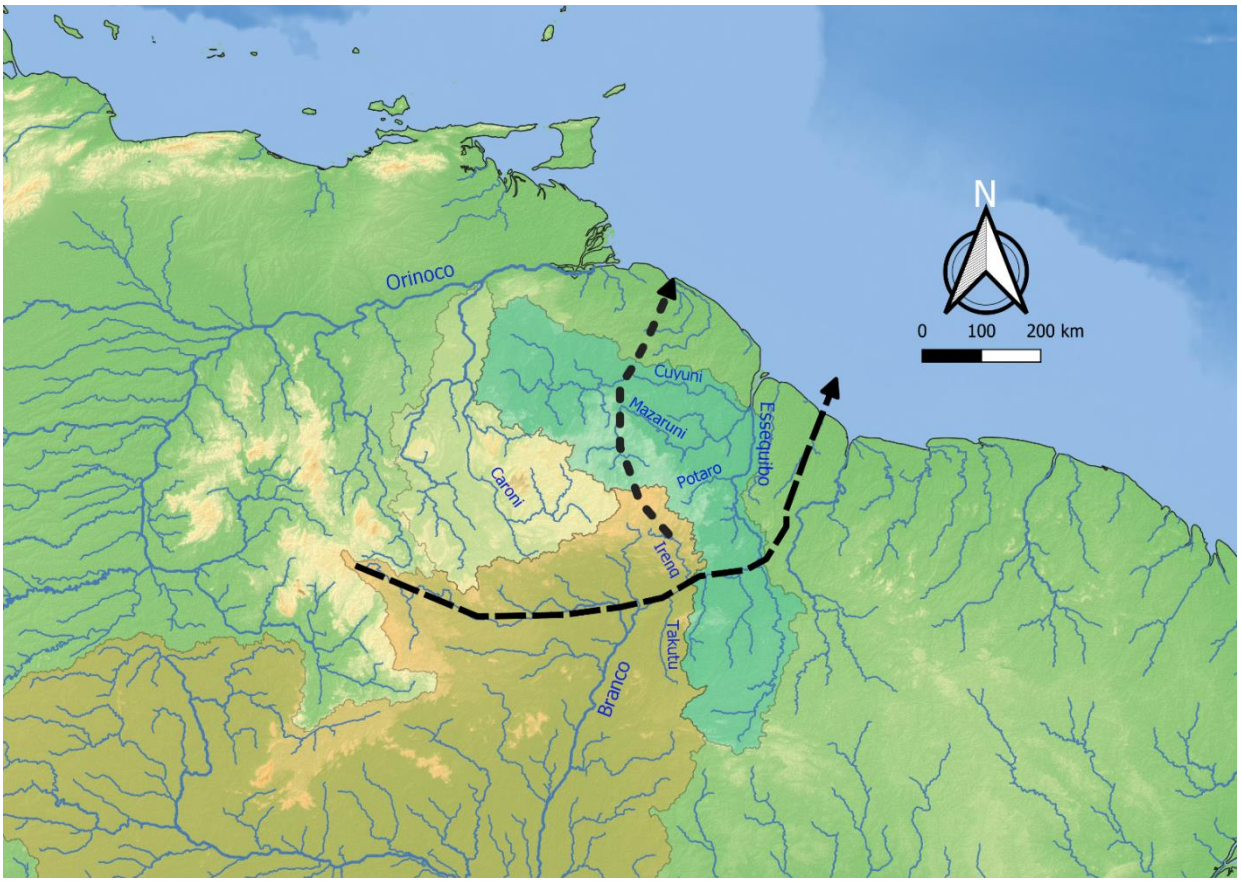

Figure 9: Trichomycterus of the Guiana Shield. A. Trichomycterus atoradorum n. sp. ROM 95880, B. T. celsae, AUM 63676, C. T. conradi, AUM 67194, D. T. cooperwiti, AUM , E. T. gransabanensis n. sp., AUM 36634, F. T. guianensis, AUM 62392, G. T. martincarteri n. sp., ROM 93515, H. T. martincarteri n. sp., ROM unknown, I. T. ovidi, AUM 62949, J and K. T. patamonorum, small spotted and large spotted morphs, AUM 62902. Scale bars, when available, located below images, 1cm. Photos by. D. Akin (A, E), J. Armbruster (B, C, F, G, J, K), N. Lujan (D), D. Taphorn, (H), and D. Werneke (I).

Table 1: Individuals used in phylogenetic analyses and associated info

Subfamily	Clade	Species	Cat #	Tissue	Country	Drainage	16S	COI	Cytb	Rag2
Trichomycterinae - Eremophilus lineage	Areolatus	*Bullockia maldonadoi*	LBP 3112	19795	Chile	Biobio (Pacific)	KY807202	KY857926	–	KY858166
Trichomycterinae - Eremophilus lineage	Areolatus	*Trichomycterus areolatus*	LBP 3118	19819	Chile	Toltén (Pacific)	KY807241	KY857964	KY858036	KY858188
Trichomycterinae - Eremophilus lineage	Areolatus	*Trichomycterus areolatus*	LBP 997	10320	Chile	Paicavi (Pacific)	KY807240	KY857963	–	KY858187
Trichomycterinae - Eremophilus lineage	Banneaui	*Trichomycterus banneaui*	LBP 19537	77971	Colombia	Magdalena	KY807279	KY858001	–	KY858218
Trichomycterinae - Eremophilus lineage	Banneaui	*Trichomycterus banneaui*	LBP 19847	77973	Colombia	Magdalena	KY807245	KY857968	–	KY858192
Trichomycterinae - Eremophilus lineage	Banneaui	*Trichomycterus ruitoquensis*	LBP 19838	77955	Colombia	Magdalena	KY807260	KY857984	–	KY858204
Trichomycterinae - Eremophilus lineage	Banneaui	*Trichomycterus* sp. 1	LBP 19842	77963	Colombia	Magdalena	KY807280	KY858002	KY858068	–
Trichomycterinae - Eremophilus lineage	Banneaui	*Trichomycterus straminius*	LBP 19834	77958	Colombia	Magdalena	KY807284	KY858006	KY858072	KY858221
Trichomycterinae - Eremophilus lineage	Banneaui	*Trichomycterus striatus*	LBP 19846	77968	Colombia	Magdalena	KY807281	KY858003	KY858069	KY858219
Trichomycterinae - Eremophilus lineage	Chapmani	*Trichomycterus* cf. *transandianus*	LBP 19844	77965	Colombia	Magdalena	KY807277	KY857999	KY858067	KY858216
Trichomycterinae - Eremophilus lineage	Chapmani	*Trichomycterus transandianus*	LBP 19845	77967	Colombia	Magdalena	KY807285	KY858007	KY858073	KY858222
Trichomycterinae - Eremophilus lineage	Guianensis	*T. cooperwiti n. sp.*	AUM 67129	AUFT 10166	Guyana	Ireng River drainage	MT025525	MT017634	–	MT017607
Trichomycterinae - Eremophilus lineage	Guianensis	*T. cooperwiti n. sp.*	AUM 67129	AUFT 10168	Guyana	Ireng River drainage	MT025526	MT017635	–	MT017608
Trichomycterinae - Eremophilus lineage	Guianensis	*T. cooperwiti n. sp.*	AUM 67129	AUFT 10169	Guyana	Ireng River drainage	MT025527	MT017636	–	MT017609
Trichomycterinae - Eremophilus lineage	Guianensis	*T. cooperwiti n. sp.*	AUM 67129	AUFT 10170	Guyana	Ireng River drainage	MT025528	MT017637	–	MT017610
Trichomycterinae - Eremophilus lineage	Guianensis	*T. cooperwiti n. sp.*	AUM 67154	AUFT 10234	Guyana	Ireng River drainage	MT025531	MT017640	–	MT017611
Trichomycterinae - Eremophilus lineage	Guianensis	*T. cooperwiti n. sp.*	AUM 67172	AUFT 10310	Guyana	Ireng River drainage	MT025534	MT017643	–	MT017613
Trichomycterinae - Eremophilus lineage	Guianensis	*T. cooperwiti n. sp.*	AUM 67179	AUFT 10276	Guyana	Ireng River drainage	MT025532	MT017641	–	MT017612
Trichomycterinae - Eremophilus lineage	Guianensis	*T. martincarteri n. sp.*	AUM 83791	ROMT 06183	Guyana	Mazaruni River drainage	MT025535	MT017644	MT017626	MT017614
Trichomycterinae - Eremophilus lineage	Guianensis	*T. martincarteri n. sp.*	AUM 83791	ROMT 06184	Guyana	Mazaruni River drainage	MT025536	MT017645	MT017627	–
Trichomycterinae - Eremophilus lineage	Guianensis	*T. ovidi n. sp.*	AUM 62949	AUFT 6596	Guyana	Potaro River drainage	MT025523	–	MT017628	MT017615
Trichomycterinae - Eremophilus lineage	Guianensis	*T. ovidi n. sp.*	AUM 62949	AUFT 6597	Guyana	Potaro River drainage	MT025524	–	MT017629	MT017616
Trichomycterinae - Eremophilus lineage	Guianensis	*T. atoradorum n. sp.*	ROM 95880	ROMT 14915	Guyana	Takutu River drainage	unacessioned	unacessioned	unacessioned	unacessioned

Trichomycterinae - Eremophilus lineage	Guianensis	*T. atoradorum n. sp.*	ROM 95880	ROMT 14922	Guyana	Takutu River drainage	unacessioned	unacessioned	unacessioned	unacessioned
Trichomycterinae - Eremophilus lineage	Guianensis	*T. atoradorum n. sp.*	ROM 95880	ROMT 14925	Guyana	Takutu River drainage	unacessioned	unacessioned	unacessioned	unacessioned
Trichomycterinae - Eremophilus lineage	Guianensis	*T. atoradorum n. sp.*	ROM 95880	ROMT 14926	Guyana	Takutu River drainage	unacessioned	–	unacessioned	unacessioned
Trichomycterinae - Eremophilus lineage	Guianensis	*T. atoradorum n. sp.*	ROM 95880	ROMT 14927	Guyana	Takutu River drainage	–	unacessioned	unacessioned	unacessioned
Trichomycterinae - Eremophilus lineage	Guianensis	*T. patamonorum n. sp*	AUM 62902	AUFT 2186	Guyana	Potaro River drainage	MT025521	MT017631	MT017617	MT017603
Trichomycterinae - Eremophilus lineage	Guianensis	*T. patamonorum n. sp*	AUM 83790	ROMT 06185	Guyana	Mazaruni River drainage	MT025537	MT017646	MT017618	–
Trichomycterinae - Eremophilus lineage	Guianensis	*T. patamonorum n. sp*	AUM 83790	ROMT 06186	Guyana	Mazaruni River drainage	MT025538	MT017647	MT017619	–
Trichomycterinae - Eremophilus lineage	Guianensis	*T. patamonorum n. sp*	AUM 89932	ROMT 12696	Guyana	Potaro River drainage	MT025539	MT017648	MT017620	MT017600
Trichomycterinae - Eremophilus lineage	Guianensis	*T. patamonorum n. sp*	AUM 91392	ROMT 15527	Guyana	Potaro River drainage	MT025540	MT017649	MT017621	MT017601
Trichomycterinae - Eremophilus lineage	Guianensis	*T. patamonorum n. sp*	AUM 91500	ROMT 15575	Guyana	Potaro River drainage	MT025541	MT017650	MT017622	MT017602
Trichomycterinae - Eremophilus lineage	Guianensis	*T. patamonorum n. sp*	LBP 17444	69015	Guyana	Potaro (Essequibo)	KY807251	KY857974	KY858043	–
Trichomycterinae - Eremophilus lineage	Guianensis	*T. conradi*	AUM 67138	AUFT 10212	Guyana	Ireng River drainage	MT025529	MT017638	–	MT017604
Trichomycterinae - Eremophilus lineage	Guianensis	*T. conradi*	AUM 67138	AUFT 10213	Guyana	Ireng River drainage	MT025530	MT017639	–	–
Trichomycterinae - Eremophilus lineage	Guianensis	*T. conradi*	AUM 67194	AUFT 10294	Guyana	Ireng River drainage	MT025533	MT017642	–	–
Trichomycterinae - Eremophilus lineage	Guianensis	*T. conradi*	AUM 91436	ROMT 15595	Guyana	Potaro River drainage	MT025542	MT017651	MT017623	MT017605
Trichomycterinae - Eremophilus lineage	Guianensis	*T. guianensis*	AUM 62932	AUFT 6563	Guyana	Potaro River drainage	–	MT017633	MT017625	MT017606
Trichomycterinae - Eremophilus lineage	Guianensis	*T. guianensis*	AUM 63677	AUFT 2110	Guyana	Potaro River drainage	MT025520	MT017630	MT017624	–
Trichomycterinae - Eremophilus lineage	*Ituglanis*	*Ituglanis amazonicus*	LBP 11003	50532	Brazil	Mamoré (Madeira)	KY807212	KY857936	KY858017	KY858175
Trichomycterinae - Eremophilus lineage	*Ituglanis*	*Ituglanis amazonicus*	LBP 16129	66849	Brazil	Tapajós (Amazonas)	KY807225	KY857948	–	KY858181
Trichomycterinae - Eremophilus lineage	*Ituglanis*	*Ituglanis boitata*	LBP 14546	60865	Brazil	Jacuí (Laguna dos Patos)	KY807272	KY857994	KY858063	–
Trichomycterinae - Eremophilus lineage	*Ituglanis*	*Ituglanis cf. amazonicus*	UFRJ 9943		Brazil	Rio Morcego	MF434082	MK123683	MK123705	–
Trichomycterinae - Eremophilus lineage	*Ituglanis*	*Ituglanis* cf. *eichhorniarum*	LBP 10777	49859	Brazil	Taquari (Paraguay)	KY807214	KY857938	KY858019	–
Trichomycterinae - Eremophilus lineage	*Ituglanis*	*Ituglanis* cf. *eichhorniarum*	LBP 1916	14038	Brazil	Paraguay (Paraná)	KY807220	KY857943	–	KY858179
Trichomycterinae - Eremophilus lineage	*Ituglanis*	*Ituglanis* cf. *eichhorniarum*	LBP 7667	36473	Brazil	Aquidauana (Paraguay)	KY807216	KY857940	KY858021	KY858177

Trichomycterinae - Eremophilus lineage	*Ituglanis*	*Ituglanis* cf. *parkoi*	LBP 5407	27103	Brazil	Jari (Amazonas)	KY807221	KY857944	KY858024	–
Trichomycterinae - Eremophilus lineage	*Ituglanis*	*Ituglanis* cf. *ramiroi*	LBP 15293	63262	Brazil	Paranã (Tocantins)	KY807276	KY857998	–	KY858215
Trichomycterinae - Eremophilus lineage	*Ituglanis*	*Ituglanis eichhorniarum*	LBP 4686	24825	Brazil	Paraguay (Paraná)	KY807215	KY857939	KY858020	KY858176
Trichomycterinae - Eremophilus lineage	*Ituglanis*	*Ituglanis goya*	LBP 17131	68592	Brazil	das Almas (Tocantins)	KY807222	KY857945	–	–
Trichomycterinae - Eremophilus lineage	*Ituglanis*	*Ituglanis goya*	LBP 17137	68599	Brazil	Dos Couros (Tocantins)	KY807223	KY857946	–	KY858180
Trichomycterinae - Eremophilus lineage	*Ituglanis*	*Ituglanis goya*	LBP 19465	77969	Brazil	das Brancas (Tocantins)	KY807278	KY858000	–	KY858217
Trichomycterinae - Eremophilus lineage	*Ituglanis*	*Ituglanis herberti*	LBP 2442	16211	Brazil	Araguaia (Tocantins)	KY807211	KY857935	KY858016	–
Trichomycterinae - Eremophilus lineage	*Ituglanis*	*Ituglanis herberti*	LBP 676	8028	Brazil	Pirai (Paraná)	KY807224	KY857947	KY858025	–
Trichomycterinae - Eremophilus lineage	*Ituglanis*	*Ituglanis parahybae*	LBP 10703	49719	Brazil	Macabú (Atlantic)	KY807219	–	KY858023	KY858178
Trichomycterinae - Eremophilus lineage	*Ituglanis*	*Ituglanis parkoi*	LBP 14153	59188	Brazil	Tapajós (Amazonas)	KY807213	KY857937	KY858018	–
Trichomycterinae - Eremophilus lineage	*Ituglanis*	*Ituglanis parkoi*	LBP 7995	37376	Brazil	Arinos (Tapajós)	KY807226	KY857949	KY858026	–
Trichomycterinae - Eremophilus lineage	*Ituglanis*	*Ituglanis* sp. n. 1	LBP 7416	35678	Brazil	Ribeira de Iguape (Atlantic)	KY807217	KY857941	KY858022	–
Trichomycterinae - Eremophilus lineage	*Ituglanis*	*T.* cf. *conradi*	AUM 51758	AUFT 4743	Suriname	Maroni River drainage	MT025522	MT017632	–	–
Trichomycterinae - Eremophilus lineage	Mutisii	*Eremophilus mutisii*	no voucher	11306	Colombia	Magdalena	KY807207	KY857931	–	KY858171
Trichomycterinae - Eremophilus lineage	Mutisii	*Trichomycterus cachiraensis*	LBP 19832	77943	Colombia	Magdalena	KY807248	KY857971	–	KY858195
Trichomycterinae - Eremophilus lineage	Mutisii	*Trichomycterus sandovali*	LBP 19833	77947	Colombia	Magdalena	KY807261	KY857985	KY858052	KY858205
Trichomycterinae - Eremophilus lineage	no clade	*Trichomycterus sp JM*	UFRJ 10736		Brazil		–	MW196746	MW196756	MW196778
Trichomycterinae - Eremophilus lineage	no clade	*Trichomycterus* sp. 2	LBP 8563	43332	Brazil	Tapajós (Amazonas)	KY807283	KY858005	KY858071	–
Trichomycterinae - Trichomycterus lineage	Brasilensis	*Trichomycterus brasiliensis*	LBP 11778	58144	Brazil	Upper São Francisco	KY807271	KY857993	KY858062	–
Trichomycterinae - Trichomycterus lineage	Brasilensis	*Trichomycterus candidus*	LBP 11630	58011	Brazil	Uberaba (Grande)	KY807242	KY857965	KY858037	KY858189
Trichomycterinae - Trichomycterus lineage	Brasilensis	*Trichomycterus* cf. *pirabitira*	LBP 2714	17464	Brazil	Grande (Paraná)	KY807287	–	KY858075	KY858224
Trichomycterinae - Trichomycterus lineage	Brasilensis	*Trichomycterus nigroauratus*	LBP 6347	29864	Brazil	Grande (Paraná)	KY807249	KY857972	KY858041	–
Trichomycterinae - Trichomycterus lineage	Brasilensis	*Trichomycterus nigroauratus*	LBP 8042	37769	Brazil	Paraiba do Sul (Atlantic)	KY807265	–	KY858056	KY858207
Trichomycterinae - Trichomycterus lineage	Brasilensis	*Trichomycterus pirabitira*	LBP 18381	72641	Brazil	Grande (Paraná)	KY807258	KY857982	KY858051	–
Trichomycterinae - Trichomycterus lineage	Brasilensis	*Trichomycterus* sp. 6	LBP 10282	47992	Brazil	Grande (Paraná)	KY807270	KY857992	KY858061	KY858212

Trichomycterinae - Trichomycterus lineage	Immaculatus	*Trichomycterus albinotatus*	LBP 6326	29802	Brazil	Paraiba do Sul (Atlantic)	KY807243	KY857966	KY858038	KY858190
Trichomycterinae - Trichomycterus lineage	Immaculatus	*Trichomycterus alternatus*	LBP 1014	10261	Brazil	Doce (Atlantic)	KY807244	KY857967	KY858039	KY858191
Trichomycterinae - Trichomycterus lineage	Immaculatus	*Trichomycterus alternatus?*	LBP 1021	10264	Brazil	Paraiba do Sul (Atlantic)	KY807250	KY857973	KY858042	KY858196
Trichomycterinae - Trichomycterus lineage	Immaculatus	*Trichomycterus* cf. *auroguttatus*	LBP 8374	40446	Brazil	Paraiba do Sul (Atlantic)	KY807268	KY857990	KY858059	KY858210
Trichomycterinae - Trichomycterus lineage	Immaculatus	*Trichomycterus* cf. *mimosensis*	LBP 8290	38358	Brazil	Jequitinhonha (Atlantic)	KY807266	KY857989	KY858057	KY858208
Trichomycterinae - Trichomycterus lineage	Immaculatus	*Trichomycterus immaculatus*	LBP 8351	40419	Brazil	Doce (Atlantic)	KY807253	KY857976	KY858045	KY858197
Trichomycterinae - Trichomycterus lineage	Immaculatus	*Trichomycterus immaculatus*	UFRJ 10001		Brazil		MF434086	MK123694	MK144348	MF431120
Trichomycterinae - Trichomycterus lineage	Immaculatus	*Trichomycterus nigricans*	UFRJ 10989		Brazil		MN385782	MN813005	MK123723	MK123765
Trichomycterinae - Trichomycterus lineage	Immaculatus	*Trichomycterus pradensis*	LBP 8291	38359	Brazil	Jequitinhonha (Atlantic)	KY807267	–	KY858058	KY858209
Trichomycterinae - Trichomycterus lineage	Itatiayae	*Trichomycterus itatiayae*	LBP 16356	62282	Brazil	Paraiba do Sul (Atlantic)	KY807254	KY857977	KY858046	KY858198
Trichomycterinae - Trichomycterus lineage	Itatiayae	*Trichomycterus pyratimbara*	LBP 9004	42138	Brazil	Grande (Paraná)	KY807247	KY857970	KY858040	KY858194
Trichomycterinae - Trichomycterus lineage	Itatiayae	*Trichomycterus reinhardti*	LBP 16302	61942	Brazil	Paraopeba (São Francisco)	KY807275	KY857997	KY858066	KY858214
Trichomycterinae - Trichomycterus lineage	Itatiayae	*Trichomycterus reinhardti*	UFRJ 9489		Brazil		MF434085	MK123698	MK123711	MF431119
Trichomycterinae - Trichomycterus lineage	Minutum	*Cambeva cf. brachykechonos*	UFRJ 10587		Brazil	Jacuí	MF434084	–	MK123711	MF431122
Trichomycterinae - Trichomycterus lineage	Minutum	*Scleronema* cf. *angustirostre*	LBP 13185	55146	Brazil	Laguna dos Patos (Atlantic)	KY807239	KY857962	–	KY858186
Trichomycterinae - Trichomycterus lineage	Minutum	*Scleronema minutum*	LBP 3310	19841	Brazil	Laguna dos Patos (Atlantic)	KY807234	KY857957	KY858031	KY858184
Trichomycterinae - Trichomycterus lineage	Minutum	*Scleronema sp 1*	UFRJ 10592		Brazil		MF434081	–	MK123709	MF431118
Trichomycterinae - Trichomycterus lineage	Minutum	*Trichomycterus cubataonis*	LBP 3123	19690	Brazil	Itapocu (Atlantic)	KY807288	KY858009	KY858076	KY858225
Trichomycterinae - Trichomycterus lineage	Minutum	*Trichomycterus davisi*	LBP 7130	34219	Brazil	Paranapanema (Paraná)	KY807264	KY857988	KY858055	–
Trichomycterinae - Trichomycterus lineage	Minutum	*Trichomycterus diatropoporos*	LBP 14694	61155	Brazil	Jacuí (Laguna dos Patos)	KY807274	KY857996	KY858065	KY858213
Trichomycterinae - Trichomycterus lineage	Minutum	*Trichomycterus iheringi*	LBP 4512	24563	Brazil	Tietê (Paraná)	KY807286	KY858008	KY858074	KY858223
Trichomycterinae - Trichomycterus lineage	Minutum	*Trichomycterus perkos*	LBP 17033	66403	Brazil	Passo Fundo (Uruguay)	KY807257	KY857981	KY858050	KY858202
Trichomycterinae - Trichomycterus lineage	Minutum	*Trichomycterus poikilos*	LBP 14693	61154	Brazil	Jacuí (Laguna dos Patos)	KY807273	KY857995	KY858064	–
Trichomycterinae - Trichomycterus lineage	Minutum	*Trichomycterus* sp. SC1	LBP 727	8276	Brazil	Itapocu (Atlantic)	KY807256	KY857979	KY858048	KY858200

Trichomycterinae - Trichomycterus lineage	Minutum	*Trichomycterus* sp. SC2	LBP 3121	19686	Brazil	Itapocu (Atlantic)	KY807255	KY857978	KY858047	KY858199
Trichomycterinae - Trichomycterus lineage	Minutum	*Trichomycterus variegatus*	LBP 10289	47222	Brazil	Santo Antônio (São Francisco)	KY807269	KY857991	KY858060	KY858211
Trichomycterinae - Trichomycterus lineage	Minutum	*Trichomycterus zonatus*	LBP 2653	17409	Brazil	Ribeira de Iguape (Atlantic)	KY807262	KY857986	KY858053	–
Trichomycterinae - Trichomycterus lineage	Punctulatus	*Trichomycterus* cf. *knerii*	LBP 18717	18717	Colombia	Meta (Orinoco)	KY807263	KY857987	KY858054	KY858206
Trichomycterinae - Trichomycterus lineage	Punctulatus	*Trichomycterus punctulatus*	ANSP 180733	903	Peru	Pisco (Pacific)	KY807259	KY857983	–	KY858203
Stegophilinae		*Henonemus punctatus*	LBP 15974	66160	Brazil	Xingu (Amazonas)	KY807209	KY857933	KY858014	KY858173
Stegophilinae		*Ochmacanthus alternus*	LBP 4351	24089	Brazil	Branco (Negro-Amazonas)	KY807210	KY857934	KY858015	KY858174
Stegophilinae		*Ochmacanthus reinhardti*	LBP 10987	50481	Brazil	Madeira (Amazonas)	KY807230	KY857953	KY858028	–
Stegophilinae		*Stegophilus panzeri.*	LBP 1858	13281	Brazil	Araguaia (Tocantins)	KY807237	KY857960	KY858034	–
Vandelliinae		*Paravandellia* sp.	LBP 1666	12749	Brazil	Negro (Amazonas)	KY807232	KY857955	KY858029	KY858183
Vandelliinae		*Vandellia cirrhosa*	LBP 3178	19329	Venezuela	Apure (Orinoco)	KY807290	KY858011	KY858077	KY858226
Vandelliinae		*Vandellia* sp. 1	LBP 15976	66164	Brazil	Xingu (Amazonas)	KY807292	KY858013	KY858079	–
Vandelliinae		*Vandellia* sp. 2	LBP 10155	47557	Venezuela	Apure (Orinoco)	KY807291	KY858012	KY858078	–

Table 2: Primers used for PCR

Loci	Primer	Primer Sequence 5'-3'	Source
16S	16Sa-L	ACGCCTGTTTATCAAAAACAT	Palumbi (1996)
	16Sb-H	CCGGTCTGAACTCAGATCACGT	Palumbi (1996)
COI	FishF1	TCAACCAACCACAAAGACATTGGCAC	Ward et al. (2005)
	FishR1	TAGACTTCTGGGTGGCCAAAGAATCA	Ward et al. (2005)
Cytb	Cytb Siluri F	CCA CCG TTG TAA TTC AAC TA	Villa-Verde et al. (2012)
	Cytb Siluri R	GAT TAC AAG ACC GGC GCT TT	Villa-Verde et al. (2012)
rag2 - step one	164F	AGCTCAAGCTGCGYGCCAT	Oliveira et al. (2011)
	RAG2-R6	TGRTCCARGCAGAAGTACTTG	Lovejoy e Collette (2001)
rag2 - step two	176R	GYGCCATCTCATTCTCCAACA	Oliveira et al. (2011)
	Rag2Ri	AGAACAAAAGATCATTGCTGGTCGGG	Oliveira et al. (2011)

Table 3: *Trichomycterus* lots used in morphological analyses, coordinates, and number of individuals per lot.

Species	Catalog#	Lat	Long	N	SL (mm)
T. atoradorum n. sp.	ROM 95880	2.811967	-59.8667	7	51.1-82.1
T. c.f. celsae	AUM 36672	4.94401	-61.121	1	36.4
T. celsae	AUM 63676	5.01888	-61.1145	1	49.4
T. conradi	AUM 67194	5.08867	-59.9695	1	44.9
T. conradi	ROM 91436	5.413959	-59.4703	9	23-41.7
T. patamonorum n. sp.	AUM 28148	5.00139	-59.6258	4	60.8-97.9
T. patamonorum n. sp.	AUM 35585	5.52519	-60.2322	5	30-53.7
T. patamonorum n. sp.	AUM 35590	5.5349	-60.2332	5	29.8-51.7
T. patamonorum n. sp.	AUM 45167	4.9668	-59.581	1	83.4
T. patamonorum n. sp.	AUM 45399	4.96667	-59.851	9	37.3-101.9
T. patamonorum n. sp.	AUM 62733	5.37608	-59.5505	13	74.6-100.3
T. patamonorum n. sp.	AUM 62742	5.37608	-59.5505	1	63.6
T. patamonorum n. sp.	AUM 62748	5.33816	-59.5663	10	58.3-72.8
T. patamonorum n. sp.	AUM 62754	5.35081	-59.5448	7	54.4-94.2
T. patamonorum n. sp.	AUM 62802	5.37608	-59.5505	10	73.9-85.3
T. patamonorum n. sp.	AUM 62812	5.36405	-59.5432	3	38-47.1
T. patamonorum n. sp.	AUM 62902	5.40532	-59.5439	14	51.5-62.7
T. patamonorum n. sp.	AUM 62910	5.30181	-59.8984	9	35.3-100.5
T. patamonorum n. sp.	AUM 62935	5.30181	-59.8984	1	34.1
T. patamonorum n. sp.	INHS 49567	5.001389	-59.6258	3	68.1-101.7
T. patamonorum n. sp.	ROM 83790	5.4755	-60.7797	6	39.8-74.3
T. patamonorum n. sp.	ROM 83804	5.48606	-60.7896	2	51.6-79.3
T. patamonorum n. sp.	ROM 89590	5.4755	-60.7767	1	54.4
T. patamonorum n. sp.	ROM 89618	5.381871	-60.7205	1	62.6
T. patamonorum n. sp.	ROM 89696	5.58132	-60.8086	1	50.7
T. patamonorum n. sp.	ROM 89716	5.381871	-60.7205	1	56.1
T. patamonorum n. sp.	ROM 89932	4.95407	-59.8588	6	64.3-93.5
T. patamonorum n. sp.	ROM 89940	4.94252	-59.8253	2	30.5-50.5
T. patamonorum n. sp.	ROM 91352	5.314144	-59.5515	18	55.7-88
T. patamonorum n. sp.	ROM 91493	5.275418	-59.7012	1	74
T. patamonorum n. sp.	ROM 93441	5.475495	-60.779	6	44-59
T. patamonorum n. sp.	ROM 93451	5.475549	-60.779	3	40-50.7
T. patamonorum n. sp.	ROM 93459	5.475693	-60.779	1	44.7
T. patamonorum n. sp.	ROM 93482	5.469784	-60.7797	1	50.4
T. patamonorum n. sp.	ROM 93511	5.486811	-60.7777	1	72.9
T. patamonorum n. sp.	ROM 93526	5.486811	-60.7777	1	38
T. patamonorum n. sp.	ROM 93539	5.486811	-60.7777	4	50.4-67.5
T. patamonorum n. sp.	ROM 94991	5.29113	-59.7192	2	44.8-59.6
T. patamonorum n. sp.	ROM 95000	5.005817	-59.6303	2	36.8-38.5
T. patamonorum n. sp.	ROM 95076	5.06263	-59.6604	1	31.6
T. patamonorum n. sp.	AUM 36615	5.74335	-61.4034	6	34.9-79

T. patamonorum n. sp.	AUM 36653	4.41422	-61.7176	1	36.5
T. patamonorum n. sp.	AUM 36680	5.03499	-60.9729	5	26.4-32.8
T. patamonorum n. sp.	AUM 36681	5.03499	-60.9729	12	22.2-54.1
T. guianensis	AUM 62932	5.30181	-59.8984	1	109.3
T. guianensis	AUM 62938	5.30436	-59.8845	1	35.9
T. guianensis	AUM 63677	5.30181	-59.8984	3	43.1-75.8
T. guianensis	ROM 78137	5.12944	-59.8103	1	20.2
T. gransabanensis n. sp.	AUM 36634	5.01888	-61.1145	4	25.6-66.5
T. martincarteri n. sp.	ROM 83791	5.4755	-60.7797	5	23.6-70.8
T. martincarteri n. sp.	ROM 83818	5.49967	-60.7776	1	70.7
T. martincarteri n. sp.	ROM 83833	5.48331	-60.7321	3	40.2-68.9
T. martincarteri n. sp.	ROM 83834	5.48331	-60.7321	2	57.6-59.7
T. martincarteri n. sp.	ROM 83842	5.48622	-60.7325	2	65-75.6
T. martincarteri n. sp.	ROM 89625	5.381871	-60.7205	1	54.5
T. martincarteri n. sp.	ROM 89627	5.381871	-60.7205	1	40.4
T. martincarteri n. sp.	ROM 89685	5.73623	-60.3596	1	36.4
T. martincarteri n. sp.	ROM 89717	5.381871	-60.7205	2	39.9-54.1
T. martincarteri n. sp.	ROM 89725	5.73488	-60.3602	1	46.7
T. martincarteri n. sp.	ROM 93437	5.475495	-60.779	2	43.4-63.3
T. martincarteri n. sp.	ROM 93441	5.475495	-60.779	2	55.2-61
T. martincarteri n. sp.	ROM 93457	5.475549	-60.779	1	61.8
T. martincarteri n. sp.	ROM 93469	5.475693	-60.779	1	42.9
T. martincarteri n. sp.	ROM 93512	5.486811	-60.7777	1	70.5
T. martincarteri n. sp.	ROM 93515	5.486811	-60.7777	4	57.4-68.1
T. martincarteri n. sp.	ROM 93539	5.486811	-60.7777	1	60.4
T. martincarteri n. sp.	ROM 93542	5.486811	-60.7777	1	72.2
T. ovidi n. sp.	AUM 62949	5.304	-59.8982	13	37.3-134.7
T. cooperwiti n. sp.	AUM 67072	4.67585	-60.0605	1	24.5
T. cooperwiti n. sp.	AUM 67098	4.71971	-60.0131	1	28.9
T. cooperwiti n. sp.	AUM 67129	5.08955	-59.9751	17	25.1-53.9
T. cooperwiti n. sp.	AUM 67138	5.04398	-59.9772	3	25.7-28.1
T. cooperwiti n. sp.	AUM 67154	5.08388	-59.9876	1	43.9
T. cooperwiti n. sp.	AUM 67172	5.08955	-59.9751	4	33-77
T. cooperwiti n. sp.	AUM 67179	5.04398	-59.9772	2	35.2-62.1
T. cooperwiti n. sp.	AUM 67200	4.96554	-59.9941	1	31

Table 4: Meristics of cleared and stained specimens and alcohol preserved specimens of Guiana Shield *Trichomycterus*.

		Modal Values (Ranges in Parentheses)								
	species	patamonorum n. sp.	celsae	conradi	atoradorum n. sp.	guianensis	cooperwiti n. sp.	martincarteri n. sp.	ovidi n. sp.	gransbanensis n. sp.
	n	8	NA	1	1	1	1	2	2	1
CS specimens	Number of vertebrae	(33-34)	NA	38	36	39	37	37	50	38
	Vertebrae post-anal	16 (15-16)	NA	17	16	19	18	17	19	18
	Vertebrae post-dorsal	21 (19-21)	NA	19	20	23	21	21	(22-23)	21
	Vertebrae post-procurrents	6 (5-7)	NA	7	7	15	12	(9-10)	(12-13)	11
	Ventral procurrents	10 (10-11)	NA	15	14	25	15	(16-17)	(18-21)	21
	Dorsal procurrents	(12-14)	NA	12	15	39	26	(21-22)	26	30
	Unsegmented dorsal rays	iii (ii-iii)	NA	iii	iii	iii	iii	iii	iii	iii
	Unsegmented anal rays	iii (ii-iii)	NA	iii	iii	iii	iii	iii	iii	iii
	n	172	1	10	6	5	29	32	12	9
Alcohol specimens	Interopercular odontodes [mean instead of mode]	42 (12-82)	26	18.5 (15-26)	43.5 (40-49)	15 (13-18)	21 (17-30)	32 (16-35)	12.5 (10-14)	13 (12-17)
	Opercular odontodes [mean instead of mode]	9 (4-14)	14	15 (14-19)	19 (18-24)	9 (9-11)	13 (10-15)	13 (8-15)	14 (12-16)	15 (9-18)
	Dorsal rays	II,7 (II-III,6-8, 0-I)	II,7	II,7 (II,6-7,0-I)	II,7 (I-II, 7)	II,7	II,7 (I-III,6-8,0-I)	II,7 (I-II,6-8)	II,5 (I-III,4-7,0-I)	II,7
	Pectoral rays	I,9 (I,7-10,0-I)	I,6	I,6 (I,5-6,0-I)	I,8 (I,8-9)	I,7	I,7 (I,6-7,0-I)	I,6 (I,6-7)	I,4 (I-II,3-4,0-I)	I,6
	Pelvic rays	I,4	I,4	I,4 (I,3-4,0-I)	I,4	I,4	I,4 (I-II,2-4,0-i)	I,4	II,1,I (II-IIII,0-1,0-I)	I,4 (I,3-4,0-I)
	Anal rays	II,5 (I-III, 4-6)	II,5	II,5 (II,4-5,0-I)	II,5	II,5 (II,5,0-I)	II,5 (I-II,4-6)	II,5 (I-III,5-6)	II,4 (II-III,4,I)	II,5
	Caudal rays	I,11,I	I,11,I	I,11,I	I,11,I (I,10-11,I)	I,11,I	I,11,I	I,11,I (0-I,9-12,I)	I,11,I (I-II,11,I)	I,11,I

Table 5: Linear measurements of *Trichomycterus atoradorum* n. sp.

	min	max	mean	SD
Standard Length	51.1	82.1		
% of Standard Length				
Body depth	14.5	18.8	16.4	1.4
Caudal Peduncle length	17.3	19.8	18.8	0.9
Caudal Peduncle depth	13.0	14.3	13.6	0.5
Predorsal length	64.4	65.9	65.3	0.5
Preanal L.	70.5	72.5	71.6	0.8
Prepelvic L.	56.1	58.2	56.9	0.9
Postdorsal L	25.8	27.8	26.8	0.8
Dorsal-fin base length	10.4	11.0	10.7	0.2
Anal-fin base length	7.2	8.6	8.0	0.5
Head L.	17.2	19.8	18.5	0.9
Head width	16.7	20.3	18.3	1.3
Head depth	9.2	10.5	10.1	0.5
Pectoral-fin length	20.3	24.8	22.9	1.8
Pectoral-short length	11.0	14.8	13.5	1.4
Pelvic-fin length	9.1	11.3	10.1	1.0
% of Head Length				
Interorbital width	30.7	37.9	34.1	2.7
Snout length	42.2	44.7	43.7	1.0
Nasal barbel length	70.5	103.6	88.0	12.0
Maxillary barbel length	80.1	96.9	91.0	6.2
Rictal Barbel length	59.4	74.8	67.5	5.9
Mouth width	32.4	41.9	38.7	3.3
Eye diameter	8.9	10.5	9.7	0.6
Interopercular odontode patch length	36.7	47.0	41.0	3.9

Table 6: Linear measurements of *Trichomycterus cooperwiti* n. sp.

	min	max	mean	SD
Standard Length	24.5	77.0		
% of Standard Length				
Body depth	12.1	23.6	17.5	2.6
Caudal Peduncle length	19.0	24.7	21.0	1.5
Caudal Peduncle depth	11.4	18.1	15.8	2.1
Predorsal length	60.7	65.8	62.7	1.4
Preanal L.	65.1	73.3	68.3	1.9
Prepelvic L.	50.2	56.4	53.1	1.4
Postdorsal L	22.9	30.0	26.7	1.7
Dorsal-fin base length	10.0	13.4	11.8	0.8
Anal-fin base length	6.2	10.6	8.8	1.0
Head L.	15.8	22.3	18.9	1.4
Head width	15.7	20.0	17.9	1.0
Head depth	9.0	11.0	10.1	0.5
Pectoral-fin length	13.9	24.9	19.1	2.7
Pectoral-short length	9.2	15.0	12.1	1.5
Pelvic-fin length	6.7	12.0	9.4	1.3
% of Head Length				
Interorbital width	24.7	38.3	30.6	3.3
Snout length	33.2	48.3	41.1	4.0
Nasal barbel length	31.0	90.6	64.8	13.7
Maxillary barbel length	39.1	92.9	70.2	10.9
Rictal Barbel length	27.0	83.5	54.5	12.9
Mouth width	31.3	51.3	38.7	4.8
Eye diameter	8.0	13.2	10.9	1.4
Interopercular odontode patch length	25.4	37.7	31.2	2.8

Table 7: Linear measurements of *Trichomycterus gransabanensis* n. sp.

	min	max	mean	SD
Standard Length	25.6	66.5		
% of Standard Length				
Body depth	14.72	16.82	15.71	1.06
Caudal Peduncle length	20.31	22.20	21.48	1.02
Caudal Peduncle depth	12.49	15.31	13.59	1.50
Predorsal length	60.58	63.51	62.10	1.47
Preanal L.	68.03	71.19	69.54	1.59
Prepelvic L.	55.93	58.00	56.86	1.05
Postdorsal L	24.74	28.38	26.70	1.84
Dorsal-fin base length	9.45	10.99	10.32	0.79
Anal-fin base length	6.52	8.02	7.43	0.80
Head L.	15.92	20.09	18.16	2.10
Head width	14.55	17.60	16.17	1.53
Head depth	9.17	9.95	9.63	0.41
Pectoral-fin length	16.48	19.22	18.24	1.53
Pectoral-short length	10.39	14.01	12.67	1.98
Pelvic-fin length	7.83	11.17	9.57	1.67
% of Head Length				
Interorbital width	26.71	30.87	28.45	2.16
Snout length	44.95	48.06	46.44	1.56
Nasal barbel length	70.94	88.79	81.13	9.19
Maxillary barbel length	79.41	95.98	85.30	9.27
Rictal Barbel length	49.29	77.38	63.16	14.05
Mouth width	33.83	40.42	36.42	3.51
Eye diameter	10.39	13.32	12.05	1.51
Interopercular odontode patch length	33.81	35.52	34.48	0.91

Table 8: Linear measurements of *Trichomycterus martincarteri* n. sp.

	min	max	mean	SD
Standard Length	23.6	75.6		
% of Standard Length				
Body depth	14.30	19.37	16.94	1.26
Caudal Peduncle length	15.73	20.90	18.46	1.29
Caudal Peduncle depth	12.52	16.77	14.59	0.96
Predorsal length	61.52	66.82	64.13	1.39
Preanal L.	67.28	74.39	71.63	1.79
Prepelvic L.	48.31	59.49	56.04	2.24
Postdorsal L	22.89	28.35	25.33	1.60
Dorsal-fin base length	8.99	13.74	11.38	0.84
Anal-fin base length	6.87	10.62	8.43	1.00
Head L.	15.35	20.95	18.28	1.46
Head width	13.38	18.70	16.06	1.08
Head depth	8.12	11.20	9.41	0.92
Pectoral-fin length	15.23	23.86	19.16	1.87
Pectoral-short length	10.44	16.47	12.60	1.27
Pelvic-fin length	6.51	11.36	9.39	1.03
% of Head Length				
Interorbital width	23.76	32.68	27.99	2.45
Snout length	40.44	52.57	46.43	3.11
Nasal barbel length	50.78	86.86	68.15	9.86
Maxillary barbel length	48.15	83.54	70.45	8.12
Rictal Barbel length	42.44	70.01	56.60	8.24
Mouth width	23.71	46.12	35.55	5.06
Eye diameter	6.64	14.64	9.93	1.85
Interopercular odontode patch length	29.89	39.89	33.73	2.54

Table 9: Linear measurements of *Trichomycterus ovidi* n. sp.

	min	max	mean	SD
Standard Length	37.3	134.7		
% of Standard Length				
Body depth	10.6	14.2	12.8	1.1
Caudal Peduncle length	18.6	21.8	20.0	0.9
Caudal Peduncle depth	10.3	12.6	11.7	0.7
Predorsal length	65.9	69.7	67.8	1.1
Preanal L.	70.6	77.0	73.4	2.0
Prepelvic L.	58.6	64.1	61.2	1.7
Postdorsal L	21.7	26.0	24.7	1.3
Dorsal-fin base length	6.7	8.9	7.5	0.7
Anal-fin base length	4.8	6.0	5.5	0.4
Head L.	10.5	16.0	12.4	1.5
Head width	10.1	12.6	11.3	0.8
Head depth	6.1	7.9	6.7	0.6
Pectoral-fin length	6.4	11.7	9.4	1.3
Pectoral-short length	4.6	7.1	5.5	0.7
Pelvic-fin length	3.3	5.7	3.9	0.7
% of Head Length				
Interorbital width	25.9	33.4	29.3	2.3
Snout length	34.5	45.0	39.3	2.9
Nasal barbel length	50.4	84.9	69.0	10.3
Maxillary barbel length	69.1	107.6	93.6	12.3
Rictal Barbel length	43.1	70.8	55.5	7.8
Mouth width	28.2	42.4	37.4	3.5
Eye diameter	7.0	11.3	8.9	1.3
Interopercular odontode patch length	21.8	28.3	25.6	2.2

Table 10: Linear measurements of *Trichomycterus patamonorum* n. sp.

	min	max	mean	SD
Standard Length	22.2	101.89		
% of Standard Length				
Body depth	11.9	20.7	16.4	1.7
Caudal Peduncle length	14.5	22.3	18.9	1.3
Caudal Peduncle depth	10.4	16.9	13.5	1.2
Predorsal length	57.3	65.8	61.3	1.6
Preanal L.	67.2	76.3	71.5	1.6
Prepelvic L.	49.6	59.5	54.8	1.8
Postdorsal L	24.8	33.8	28.8	1.6
Dorsal-fin base length	9.1	14.1	11.4	1.0
Anal-fin base length	5.5	11.6	8.1	1.0
Head L.	15.8	26.4	19.4	1.9
Head width	15.7	23.3	19.0	1.2
Head depth	7.9	13.3	10.2	1.0
Pectoral-fin length	14.4	28.1	20.1	2.1
Pectoral-short length	11.6	19.6	15.4	1.4
Pelvic-fin length	9.5	14.9	11.4	0.9
% of Head Length				
Interorbital width	22.2	37.0	29.2	2.6
Snout length	35.3	55.1	46.3	3.9
Nasal barbel length	40.1	98.5	63.5	9.2
Maxillary barbel length	20.9	110.7	51.6	11.1
Rictal Barbel length	15.4	67.7	38.3	7.6
Mouth width	25.8	52.7	35.4	4.8
Eye diameter	6.8	17.2	11.2	2.1
Interopercular odontode patch length	27.4	65.1	48.5	6.4

Supplementary Table 1

	T. conradi				*T. guianensis*			
% of SL	min	max	mean	SD	min	max	mean	SD
Caudal Peduncle length	16.61	18.91	17.55	0.669	19.45	23.44	21.82	1.628
Caudal Peduncle depth	9.61	12.53	10.87	0.959	14.70	17.30	16.16	1.167
Postdorsal L	21.77	24.48	23.45	0.915	26.68	30.96	27.94	1.846
% of Head Length	min	max	mean	SD	min	max	mean	SD
Nasal barbel length	50.11	76.53	63.37	7.731	92.17	101.70	96.97	4.413
Maxillary barbel length	45.15	81.96	68.99	10.985	89.12	119.04	107.07	13.572
Rictal Barbel length	42.39	56.13	48.22	3.915	78.44	96.55	83.90	7.310